

Boundary layers and universal distribution in boundary driven active systems

Pritha Dolai^{1,2,3} † and Arghya Das^{4*}

¹ National Institute of Technology Karnataka Surathkal, Mangalore 575025, India

² Friedrich-Alexander-Universität Erlangen-Nürnberg, Erlangen 91054, Germany

³ Max-Planck-Zentrum für Physik und Medizin, Erlangen 91058, Germany

⁴ The Institute of Mathematical Sciences, Taramani, Chennai, 600113, India

†pritha@nitk.edu.in, *arghyaburo21@gmail.com

Abstract

We study non-interacting run-and-tumble particles (RTPs) in one dimension driven by particle reservoirs at the boundaries. Analytical results for the steady state and dynamics are obtained and new active features are observed. In steady state, a Seebeck-like effect is identified. The spatial and internal degrees of freedom, combined together, possess a symmetry, using which we found the eigenspectrum for large systems. The eigenvalues are arranged in two distinct bands. There is a crossover from system size-independent relaxation rate to the diffusive relaxation as the system size is increased. The time-dependent distribution is calculated and extended to the semi-infinite line. In the dynamics, a ‘Milne length’ emerges that depends non-trivially on diffusivity and other parameters. Notably, the large time distribution retains a strong and often dominant ‘active’ contribution in the bulk, implying that an effective passive-like description is inadequate. We report the existence of a ‘kinetic boundary layer’ both in the steady-state and time-dependent regime, which is a consequence of thermal diffusion. In the absorbing boundary problem, a novel universality is proposed when the particle is driven by short-ranged colored noise.

The authors contributed equally to the project.

1 Introduction

Systems with self-propelled or active particles became a paradigm of non-equilibrium processes. Active agents consume energy from environment and convert it into mechanical work to propel themselves. Constant energy consumption drives active systems out of equilibrium [1, 2, 3]. There are numerous real life examples of active systems across scales including bacterial colony, school of fish, flock of birds, janus particles [4, 5], vibrated granular rods and beads [6, 7] and many more. Such systems exhibit a plethora of non-trivial collective phenomena, e.g. pattern formation, motility-induced phase separation and clustering [2, 3, 8, 9, 10], giant number fluctuations [11], casimir effect [12]. They reveal rich nonequilibrium properties even at the single particle level: Examples include non-Boltzmann steady-state, accumulation near boundary, shape transition in probability distribution in a trapping potential, and so on [13, 14, 15, 16]. Active motion is modelled with a Langevin-like equation with an ‘active noise’, which is typically coloured and violates the fluctuation-response relation, leading to novel far from equilibrium behaviour. In literature there are three broad classes of scalar active particle models depending on the nature of the active noise: run-and-tumble particles (RTP), active Brownian particles (ABP) and active-Ornstein-Uhlenbeck particles (AOUP).

Active particles show interesting behaviour in the presence of drives, thermal noise, obstacles and different boundary conditions. For example, RTPs subject to spatially periodic drive go through a transition from non-ergodic trapped states to moving states [17]. In presence of shear forces in two dimension, underdamped ABPs develop a boundary layer and flow reversal occurs near the wall [18]. Confining boundaries are known to have strong effects on active systems, e.g. boundary accumulation and boundary layer formation [13, 19], long-range effects and system size dependent behaviour [20, 21, 22, 23, 24, 25], etc. Interestingly, the nature of the boundary layer and the pressure exerted by the particles on an obstacle or a wall depends on the shape of the wall [19] as well as on the inter-particle and particle-wall interaction [20]. Thermal fluctuations, ubiquitous but usually neglected, can have nontrivial effects on active motion e.g. formation of bound states [26], current modulation on a ratchet [27], and phase separation [28, 29].

In the current work, we focus on boundary-driven processes. Systems connected to particle or energy reservoirs have been studied for centuries, but there is a renewed interest in boundary driven processes particularly in context to low dimensional transport. The usual behaviour of such a system is modelled by Brownian particles moving in a finite system connected to particle baths: The steady state density

profile is given by a linear interpolation of the densities at the boundaries [30] while the current depends linearly on the density gradient as given by the Fick's law. However in the presence of interaction, bulk drive, or more than one conserved quantities etc. richer and often nonintuitive behaviour is observed. Simple models of boundary driven interacting diffusive systems exhibit long ranged correlation [31, 32]; introduction of a bulk drive gives rise to complex phases [33, 34]. The transport properties become anomalous and violate Fick's law in one dimensional interacting anharmonic chains [35, 36, 37]. Nonlinear bulk density profile and nongradient steady state current emerges in simpler cases where the single particle dynamics is governed by strongly correlated noise, for instance noninteracting Levy walk connected to particle reservoirs [37, 38]. New effects induced by 'active heat baths' in the energy transport and steady state properties of an otherwise passive system have also been reported recently [39, 40]. However, active systems in presence of boundary reservoirs are relatively less studied [41]. It is natural to ask what are the steady state, transport properties, dynamical fluctuations and relaxation behaviour of different boundary driven active processes and how do they differ across models and from their passive counterpart.

In this paper, we study one-dimensional non-interacting RTPs in presence of thermal noise with the system connected to particle reservoirs at both ends maintaining fixed particle densities and magnetisation ¹. The exact steady state and large time distribution are analytically obtained. The results show the existence of a 'kinetic boundary layer' characterised by exponentially decaying component(s) in the density profile near the boundaries. For zero boundary magnetisation, the steady state current and density approximate a passive-like behaviour in the bulk while the effect of activity, notable for large persistence, becomes prominent at the boundary layer. The signature of activity however does appear in the bulk through a finite magnetisation. Remarkably, when the boundary magnetisations are nonzero, a Seebeck-like effect is identified, with boundary magnetisations taking the role of temperatures and density differences being analogous to voltage differences.

The boundary value problem for the time dependent solution is identical to the absorbing boundary problem, which endows the system with a 'reflection symmetry'. Using this, the eigenspectrum and complete time dependent solutions are obtained analytically for large system-sizes. The eigenvalues of the time evolution operator is arranged in two distinct bands separated by the tumble rate. For small systems the relaxation rate is independent of the system-size L , which crosses over to diffusive

¹Since the RTPs carry two internal states in 1-dimension, the magnetisation is the difference of densities of the two species.

relaxation when L becomes large. We observe that in each of the eigenstate the ‘active’ contribution appears as $O(L^{-1})$ correction to the leading ‘passive-like’ term for large L ; but in the full solution both the active and passive contributions occur at the same order, a result that goes over to the semi-infinite case. For higher persistence, the late time distribution and related properties are in fact dominated by the active contribution. Interestingly, the ‘Milne length’ that depends non-trivially on the diffusivity and other dynamical parameters is present in the distribution. We found rather non-intuitively that the Milne length has a significant presence in the the steady state current. The kinetic boundary layer appears in the time dependent solution as well, which is argued to be a consequence of thermal diffusion. We further argue that in the semi-infinite limit this is related to a net imbalance of the two species of particles in the system, which goes away as soon as the diffusivity vanishes. As a whole, the interplay of thermal noise and active motion causes important ramifications in the dynamics.

It turns out that many of the features obtained for RTPs also appear in the underdamped passive dynamics, athermal AOUP and ABP, and are possibly generic to dynamics driven by coloured noise. In the absorbing boundary problem kinetic boundary layer was noted earlier for the underdamped passive motion [42, 43, 44]. The large time density profile in that problem is in fact quantitatively similar to that obtained for RTP. It prompts us to propose that the late time distribution away from the absorbing wall is independent of the realisation of the coloured noise, provided the noise correlation is short ranged.

The paper is organized as follows. In Section 2, we describe the model system of a boundary-driven run-and-tumble particles. The steady-state and the time dependent solutions are presented in Sections 3 and 4, respectively. A universality in the late time distribution is proposed in Section 5. We conclude in Section 6.

2 Model: boundary driven RTPs

We consider a run-and-tumble particle (RTP) moving in a finite one-dimensional box of length L subject to a translational noise $\eta(t)$. The box is connected to particle reservoirs at the two ends. We assume that the microscopic details of the interaction of the reservoir with the system at the boundary is not important except that it provides a fixed boundary condition. The schematic of the system is shown in Figure 1.

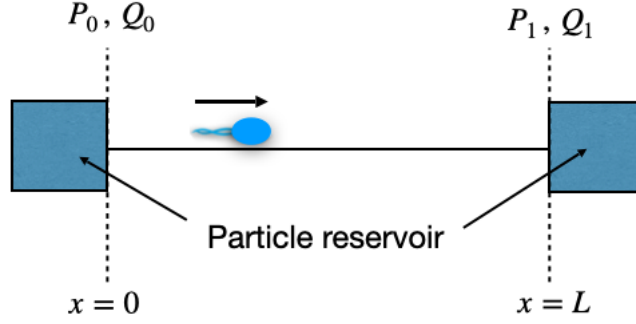


Figure 1: Schematic of the boundary driven active system. Each RTP moves on a one-dimensional line bounded between $x = 0$ and L . The system is connected to particle reservoirs at both the ends maintaining fixed particle densities P_0 and P_1 and the corresponding particle magnetisation Q_0 and Q_1 at $x = 0, L$ respectively.

The equation of motion of the particle is,

$$\dot{x} = v\sigma(t) + \eta(t), \quad (1)$$

where v is the self-propulsion speed, $\sigma(t)$ is the intrinsic orientation (spin) characterized by a telegraphic noise that takes values ± 1 and it flips between the two states with rate ω , and $\eta(t)$ is the Gaussian white noise with $\langle \eta(t) \rangle = 0$, $\langle \eta(t)\eta(t') \rangle = 2D\delta(t - t')$, D being the diffusion constant.

The state of the particle at a time t is given by, $|P(x, t)\rangle = (P_+(x, t), P_-(x, t))^T$, where $P_+(x, t)$ and $P_-(x, t)$ are the probabilities to find a particle at x at time t with instantaneous spin $+1$ and -1 respectively. P_+ and P_- satisfy the equations,

$$\partial_t P_+ = D\partial_x^2 P_+ - v\partial_x P_+ - \omega P_+ + \omega P_-, \quad (2a)$$

$$\partial_t P_- = D\partial_x^2 P_- + v\partial_x P_- + \omega P_+ - \omega P_-, \quad (2b)$$

with the boundary conditions,

$$\begin{aligned} P_+(0, t) &= P_0^+, \quad P_-(0, t) = P_0^-; \\ P_+(L, t) &= P_1^+, \quad P_-(L, t) = P_1^-. \end{aligned} \quad (3)$$

P_0^\pm and P_1^\pm are the probability densities of each species of particles at the two boundaries $x = 0$ and $x = L$ respectively. The total probability density is $P(x, t) = P_+(x, t) + P_-$. We also define a quantity $Q(x, t) := \langle \sigma \rangle_{(x, t)} = P_+(x, t) - P_-(x, t)$ which is analogous to magnetization density.

3 Steady state distribution

In the steady state $\partial_t P_{\pm} = \partial_t P_{\mp} = 0$. Using the definitions of P and Q , the equations for the steady state can be written as,

$$\partial_t P = D\partial_x^2 P - v\partial_x Q = 0 \quad (4)$$

$$\partial_t Q = D\partial_x^2 Q - v\partial_x P - 2\omega Q = 0. \quad (5)$$

For arbitrary densities of the two species of particles at each of the boundaries, we need to solve Eqs. (4)-(5) with general boundary values of $P(x)$ and $Q(x)$,

$$\begin{aligned} \text{At } x = 0 : P(0) &= P_0, Q(0) = Q_0, \\ \text{At } x = L : P(L) &= P_1, Q(L) = Q_1. \end{aligned} \quad (6)$$

The solution for the density-magnetisation profiles and the current in the steady state are,

$$\begin{aligned} P(x) = P_0 + M \left[B_0 - \Delta Q \frac{e^{-\mu L} (1 + e^{-\mu L})}{(1 - e^{-\mu L})^2} \right] + \frac{\Delta P - M(Q_0 + Q_1)}{M\frac{v}{\omega} + L} x \\ - \frac{v}{\mu D} \frac{B_0(e^{-\mu x} - e^{-\mu(L-x)}) - \Delta Q e^{-\mu(L-x)}}{1 + e^{-\mu L}}, \end{aligned} \quad (7)$$

$$Q(x) = -\frac{\Delta P - M(Q_0 + Q_1)}{2(M + L\frac{\omega}{v})} + \frac{B_0(e^{-\mu x} + e^{-\mu(L-x)}) + \Delta Q e^{-\mu(L-x)}}{1 + e^{-\mu L}}, \quad (8)$$

$$J_0 = -\frac{D_e}{M\frac{v}{\omega} + L}(\Delta P - M(Q_0 + Q_1)), \quad (9)$$

where, $\Delta P = P_1 - P_0$, $\Delta Q = Q_1 - Q_0$, $\mu = \frac{\sqrt{2\omega D_e}}{D}$, $D_e = D + \frac{v^2}{2\omega} = \frac{D^2\mu^2}{2\omega}$, $M = \frac{v}{\mu D} \frac{1 - e^{-\mu L}}{1 + e^{-\mu L}}$, and $B_0 = \frac{\Delta P - M(Q_0 + Q_1)}{2(M + L\frac{\omega}{v})} + Q_0 - \Delta Q \frac{e^{-\mu L}}{1 - e^{-\mu L}}$.

The density profile in presence of boundary magnetisation is quite nontrivial and develops nonmonotonicities near the boundaries. The distribution and magnetisation are shown in Figure 2. We list a few observations:

- I. $M \approx \frac{v}{\sqrt{2\omega D_e}}$ at large L , for which the denominator in the expression for the current is just $L + 2l_M$, where $l_M = \frac{v^2}{2\omega\sqrt{2\omega D_e}}$ is the Milne length as discussed later. This increase in the effective length resembles the absorbing conditions beyond the boundaries at $x = 0$ and L .

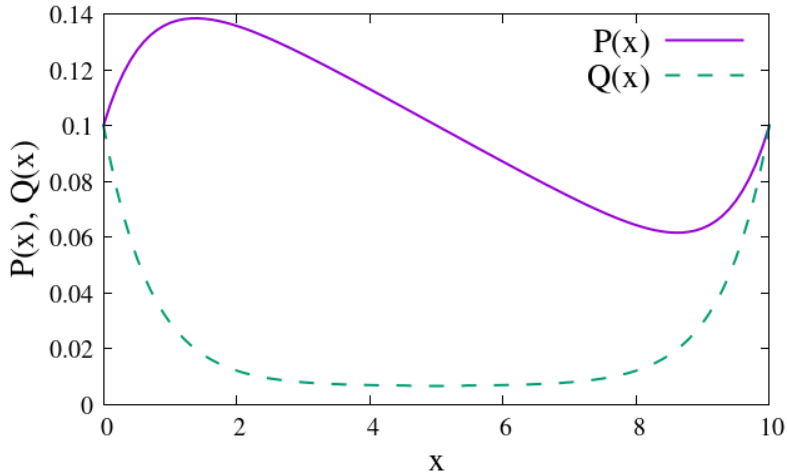


Figure 2: Steady state density and magnetisation profiles for the boundary driven RTP with nonzero boundary magnetisation. Here $v = 1.0, D = 1.0, w = 1.0, L = 10.0$ and $P_0 = P_1 = 0.1, Q_0 = Q_1 = 0.1$.

- II. The current is finite even if $\Delta P = 0$, $J_0 \propto (Q_0 + Q_1)/(L + 2l_M)$. This is suggestive that the boundary magnetisations effectively act as drives inducing a constant current in the system in absence of a density gradient. However this similarity cannot be exact, since in the present case the current gives rise to a linear density profile away from the boundaries, unlike the usual driven passive case in which density remains uniform.
- III. On the contrary, with suitable boundary magnetisations such that $Q_0 + Q_1 = \Delta P/M$, the current can actually be made to vanish without invoking any external bias to counteract the density gradient. In large systems this leads to a uniform density and almost vanishing magnetisation in the bulk ($\mu^{-1} \ll x \ll L$) and the inhomogenities remain only in the boundary layers. Imposing an additional condition of zero density gradient ($\Delta P = 0$) mimics the steady state result for reflecting boundaries [13].

To our knowledge these are some new features which might be more general for boundary driven active systems. In particular, in the zero current condition the nonzero boundary magnetisations induce a global density difference, $\Delta P = M(Q_0 + Q_1)$. This phenomenon is reminiscent of the Seebeck effect with coefficient M .

3.1 Steady state result for zero boundary magnetisation:

For the special case $P_0^+ = P_0^- = \frac{P_0}{2}$ and $P_1^+ = P_1^- = \frac{P_1}{2}$, i.e. $Q_0 = 0$, $Q_1 = 0$ [45], the solution reduces to a simpler form,

$$P(x) = P_0 + \frac{\Delta P}{\mathcal{Z}} \left[\frac{2\omega}{v}(1 + e^{-\mu L})x - \frac{v}{\mu D}(e^{-\mu x} - e^{-\mu(L-x)} - 1 + e^{-\mu L}) \right], \quad (10)$$

$$Q(x) = \frac{\Delta P}{\mathcal{Z}} [e^{-\mu x} + e^{-\mu(L-x)} - 1 - e^{-\mu L}], \quad \text{and} \quad (11)$$

$$J_0 = -\frac{D_e}{M\frac{v}{\omega} + L} \Delta P. \quad (12)$$

Here \mathcal{Z} is a constant given by,

$$\mathcal{Z} = \frac{2\omega}{v} L(1 + e^{-\mu L}) + \frac{2v}{\mu D} (1 - e^{-\mu L}). \quad (13)$$

The equations for the steady state and the boundary conditions for the boundary driven RTP are related to the exit probability $E_{\pm}(x)$ of the particle at the left boundary starting at an initial position x with initial spin ± 1 . More details are in Appendix A. It gives a simple simulation scheme for the steady state. The data with zero boundary magnetisation is shown in Figure 3, which agrees with the theoretical expressions in Eqs. (10)-(11).

We observe that, the probability of finding the particle in the system is, $\int_0^L P(x) dx = \frac{P_0 + P_1}{2} L$, which is identical to that of a passive particle. This also constrains P_0 and P_1 (and therefore ΔP) values to $O(L^{-1})$ or less, since the total probability cannot exceed 1. Further, in the $D = 0$ case μ diverges and the density and magnetisation profiles develop discontinuities at the boundaries, which is smoothed by ‘kinetic boundary layers’ as soon as a thermal noise is switched on. Emergence of the boundary layers in the open boundary problem will be discussed later.

Large- L limit: For $L \gg \frac{v}{\omega}, \mu^{-1}$, the particle undergoes many tumble events and we expect the behaviour to be largely diffusive with effective diffusion constant D_e . In this limit the steady state results can be quite accurately approximated as,

$$J_0 \simeq -D_e \frac{\Delta P}{L + 2l_M}, \quad (14)$$

$$P(x) \simeq P_0 + \frac{\Delta P}{L + 2l_M} (x + l_M) - \frac{\Delta P}{L + 2l_M} l_M (e^{-\mu x} - e^{-\mu(L-x)}), \quad (15)$$

$$Q(x) \simeq -\frac{\Delta P}{L + 2l_M} \frac{v}{2\omega} (1 - e^{-\mu x} - e^{-\mu(L-x)}), \quad (16)$$

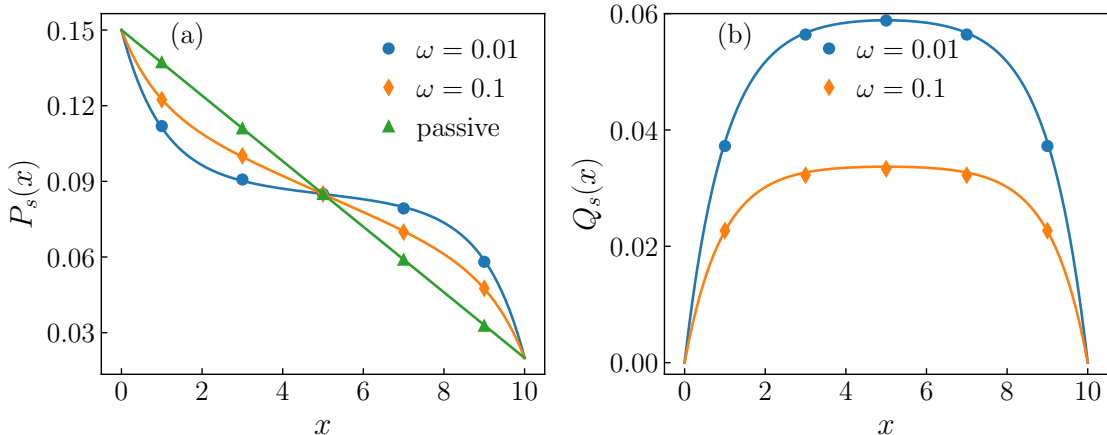


Figure 3: Steady state behaviour for the boundary driven single RTP– (a): the probability density; (b): magnetisation for different tumble rate ω . Here $L = 10$, $v = 1.0$, $D = 1.0$ and the boundary densities are $P_0 = 0.15$, $P_1 = 0.02$. Points are obtained by simulating the exit probabilities and using Eq. (82).

where l_M is the Milne length [46]. The expressions suggest that the current and density in the bulk are passive-like with a slightly larger effective system size, whereas the signature of activity shows up at the boundary layer. Nontrivial effect of activity appears in the bulk through $Q(x)$, for which there is no passive analogue and which assumes a constant value for $\mu^{-1} \ll x \ll L$.

4 Eigenspectrum and the time-dependent solution

In terms of the state vector $|P(x, t)\rangle = \begin{bmatrix} P_+(x, t) \\ P_-(x, t) \end{bmatrix}$ the evolution of the distribution of the RTP, given by the master equation (2a)-(2b), can be rewritten as,

$$\partial_t |P(x, t)\rangle = \mathcal{L} |P(x, t)\rangle, \quad (17)$$

\mathcal{L} being a linear operator,

$$\mathcal{L} = \begin{bmatrix} D\partial_x^2 - v\partial_x - \omega & \omega \\ \omega & D\partial_x^2 + v\partial_x - \omega \end{bmatrix}. \quad (18)$$

Since the run and tumble motion described in terms of $(x(t), \sigma(t))$ is a Markov process, the state vector $|P(x, t)\rangle$ can be expanded in terms of the eigenfunctions

$|\phi_n(x)\rangle$ of the time evolution operator \mathcal{L} ,

$$|P(x, t)\rangle = |P_{\text{ss}}(x)\rangle + \sum_{n=1}^{\infty} c_n e^{\lambda_n t} |\phi_n(x)\rangle, \quad (19)$$

where $|\phi_n(x)\rangle \equiv [\phi_n^+(x), \phi_n^-(x)]^T$. Substituting Eq. (19) in Eq. (17) and using the linear independence of $e^{\lambda_n t}$'s for different λ_n 's, we find,

$$\mathcal{L}|\phi_n(x)\rangle = \lambda_n |\phi_n(x)\rangle. \quad (20)$$

Here the λ_n 's are the eigenvalues of \mathcal{L} with corresponding eigenfunctions $|\phi_n(x)\rangle$ satisfying the boundary conditions $|\phi_n(0)\rangle = |\phi_n(L)\rangle = 0$ as we shall argue soon. The coefficients c_n are determined from the initial condition. Therefore, given an initial condition, the time evaluation of the system is completely determined through Eq. (19).

Let us consider the eigenfunctions $|\phi_n(x)\rangle$ to be of the form,

$$|\phi_n(x)\rangle = \alpha_n e^{k_n x} |A_n\rangle \quad (21)$$

where $|A_n\rangle = [A_n^+, A_n^-]^T$. Using the above, Eq. (20) can be written as,

$$M(k_n)|A_n\rangle = \lambda_n |A_n\rangle \quad (22)$$

with

$$M(k_n) = \begin{bmatrix} Dk_n^2 - vk_n - \omega & \omega \\ \omega & Dk_n^2 + vk_n - \omega \end{bmatrix}. \quad (23)$$

The eigenvalues of $M(k_n)$ gives the 'dispersion relation':

$$\lambda_n = -(\omega - Dk_n^2) \pm \sqrt{\omega^2 + v^2 k_n^2}. \quad (24)$$

To facilitate the subsequent analysis we invert the above relation and express k_n in terms of λ_n ,

$$k_n^2 = \frac{\lambda_n}{D} + \frac{\omega D_e}{D^2} \pm \sqrt{\left(\frac{\lambda_n}{D} + \frac{\omega D_e}{D^2}\right)^2 - \frac{\lambda_n^2 + 2\omega\lambda_n}{D^2}}, \quad (25)$$

Denoting the positive roots for the k_n 's corresponding to plus and minus sign by k_a and k_b respectively, Eq. (25) implies that there are four k_n values for each λ_n ,

$$k_n^{(1)} = k_a(\lambda_n), \quad k_n^{(2)} = -k_a(\lambda_n) \quad (26a)$$

$$k_n^{(3)} = k_b(\lambda_n), \quad k_n^{(4)} = -k_b(\lambda_n). \quad (26b)$$

The corresponding eigenvectors of $M(k_n)$ are

$$|A_n^{(i)}\rangle = \begin{bmatrix} a(k_n^{(i)}) \\ 1 \end{bmatrix}, i = 1, \dots, 4 \text{ with} \quad (27)$$

$$a(k) = (\lambda + \omega - kv - Dk^2)/\omega. \quad (28)$$

Note that, $a(k_n^{(1)})a(k_n^{(2)}) = a(k_n^{(3)})a(k_n^{(4)}) = 1$. Therefore, each eigenvalue λ_n is four-fold degenerate and the corresponding eigenfunction $|\phi_n(x)\rangle$ can be written as a linear combination:

$$|\phi_n(x)\rangle = \sum_{i=1}^4 \alpha_n^i e^{k_n^{(i)}x} |A_n^i\rangle. \quad (29)$$

The full time dependent solution for the probability distribution then becomes,

$$|P(x, t)\rangle = |P_{ss}(x)\rangle + \sum_{n=1}^{\infty} c_n e^{\lambda_n t} \sum_{i=1}^4 \alpha_n^i e^{k_n^{(i)}x} |A_n^i\rangle. \quad (30)$$

The task is to determine λ_n 's and α_n^i 's in terms of the parameters governing the dynamics, viz v , ω , D and the system size L . Recall the boundary conditions from Eq. (3),

$$\begin{aligned} |P(0, t)\rangle &= \begin{bmatrix} P_0^+/2 \\ P_0^-/2 \end{bmatrix} = |P_{ss}(0)\rangle, \\ |P(L, t)\rangle &= \begin{bmatrix} P_1^+/2 \\ P_1^-/2 \end{bmatrix} = |P_{ss}(L)\rangle. \end{aligned} \quad (31)$$

The above imply that, at $x = 0$, $|P(0, t)\rangle - |P_{ss}(0)\rangle = 0$, and similar at $x = L$. In fact, $|P_{tr}(x, t)\rangle \equiv |P(x, t)\rangle - |P_{ss}(x)\rangle$ satisfies the masters equation (2a)-(2b) but with the boundary conditions $|P_{tr}(0, t)\rangle = |P_{tr}(L, t)\rangle = 0$. Consequently, $\sum_{n=1}^{\infty} c_n e^{\lambda_n t} |\phi_n(0)\rangle = \sum_{n=1}^{\infty} c_n e^{\lambda_n t} |\phi_n(L)\rangle = 0$ at all times. Using the linear independence of $e^{\lambda_n t}$'s once again, we find, for each n ,

$$|\phi_n(0)\rangle = |\phi_n(L)\rangle = 0. \quad (32)$$

The time dependent behaviour of the boundary driven case is therefore identical to that of the one-dimensional dynamics with two absorbing ends at $x = 0$ and L . Henceforth, we shall omit the steady state. Using the absorbing boundary conditions

in Eq.(29), we get the following set of equations for the coefficients α_n^i :

$$x = 0 : \quad \sum_{i=1}^4 \alpha_n^i = 0, \quad \sum_{i=1}^4 \alpha_n^i a_n^i = 0 \quad (33a)$$

$$x = L : \quad \sum_{i=1}^4 \alpha_n^i e^{k_n^{(i)}L} = 0, \quad \sum_{i=1}^4 \alpha_n^i e^{k_n^{(i)}L} a_n^i = 0 \quad (33b)$$

where $a_n^i \equiv a(k_n^{(i)})$. Above equations can be re-written as a matrix equation, $S(k_n^{(i)})|\alpha\rangle = 0$, where $|\alpha\rangle = [\alpha_n^{(1)}, \alpha_n^{(2)}, \alpha_n^{(3)}, \alpha_n^{(4)}]^T$ and

$$S = \begin{bmatrix} 1 & 1 & 1 & 1 \\ a_n^1 & a_n^2 & a_n^3 & a_n^4 \\ e^{k_n^{(1)}L} & e^{k_n^{(2)}L} & e^{k_n^{(3)}L} & e^{k_n^{(4)}L} \\ a_n^1 e^{k_n^{(1)}L} & a_n^2 e^{k_n^{(2)}L} & a_n^3 e^{k_n^{(3)}L} & a_n^4 e^{k_n^{(4)}L} \end{bmatrix} \quad (34)$$

To have a non-trivial solution for α 's we must have

$$\det[S] = 0, \quad (35)$$

which, upon solving, determines λ_n 's as a function of system parameters. We observe that, $\lambda = 0, -2\omega$ satisfies the above determinant equation. $\lambda = 0$ stands for the steady state which is just zero for the absorbing boundaries and is discarded.

4.1 Symmetries of the model and solution for the spectrum

The determinant equation (35) is a complicated transcendental equation and we cannot find explicit solutions in general. However, the problem can be greatly simplified. Note that, the master equation (17) satisfies a *symmetry*, that is, whenever the spin is reversed ($\sigma \rightarrow -\sigma$) along with $x \rightarrow L - x$, the equation and the boundary conditions remain invariant. To express it mathematically, let us define an operation \mathcal{O}_x :

$$\mathcal{O}_x[P^+(x), P^-(x)]^T = [P^-(L-x), P^+(L-x)]^T, \quad (36)$$

as shown in Figure 4. We find that, \mathcal{O}_x commutes with \mathcal{L} , i.e. it is a symmetry operation. It also satisfies $\mathcal{O}_x^2 = I$, implying that its eigenvalues are $o_x = \pm 1$. Consequently, the eigenstates $|\phi_n(x)\rangle$ of the operator \mathcal{L} will also be an eigenstate of \mathcal{O}_x corresponding to an eigenvalue ± 1 . In the following, we segregate all the eigenstates $|\phi_n(x)\rangle$ into two symmetry sectors labelled by the values of o_x , and determine the spectrum for each of the sectors.

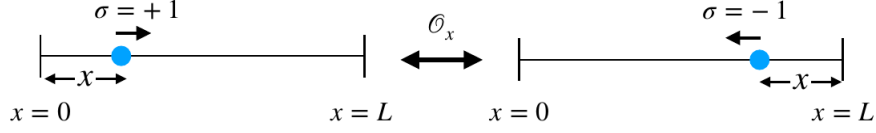


Figure 4: The symmetry of the dynamics. The master equations and the boundary conditions remain invariant under $\sigma \rightarrow -\sigma$ along with $x \rightarrow L - x$.

spectrum for $o_x = 1$ (even sector):

Here, $\phi_n^+(x) = \phi_n^-(L - x)$. Using Eq. (29) and the values of k_n 's from Eq. (26), we find,

$$\alpha^{(1)} a^{(1)} e^{k_a x} + \alpha^{(3)} a^{(3)} e^{k_b x} + \alpha^{(2)} a^{(2)} e^{-k_a x} + \alpha^{(4)} a^{(4)} e^{-k_b x} \quad (37)$$

$$= \alpha^{(1)} e^{k_a (L-x)} + \alpha^{(3)} e^{k_b (L-x)} + \alpha^{(2)} e^{-k_a (L-x)} + \alpha^{(4)} e^{-k_b (L-x)}. \quad (38)$$

We dropped the suffix n for convenience. Comparing the coefficients of each independent spatial modes $e^{k^{(i)}x}$, we obtain,

$$\alpha^{(1)} a^{(1)} = \alpha^{(2)} e^{-k_a L} \quad (39)$$

$$\alpha^{(3)} a^{(3)} = \alpha^{(4)} e^{-k_b L} \quad (40)$$

Using the above expressions in Eqs. (33) for the coefficients $\alpha^{(i)}$, we obtain,

$$\frac{\alpha^{(1)}}{\alpha^{(3)}} = -\frac{1 + a^{(3)} e^{k_b L}}{1 + a^{(1)} e^{k_a L}} = -\frac{a^{(3)} + e^{k_b L}}{a^{(1)} + e^{k_a L}}. \quad (41)$$

Rearranging the last equality we get,

$$\frac{e^{-k_b L} - e^{-k_a L}}{1 - e^{-k_a L} e^{-k_b L}} = \frac{a^{(3)} - a^{(1)}}{a^{(3)} a^{(1)} - 1}. \quad (42)$$

Here $k_a, k_b, a^{(1)}, a^{(3)}$ are all functions of λ . By solving the above expression, we can in principle find the λ 's in this sector.

spectrum for $o_x = -1$ (odd sector):

Here, $\phi_n^+(x) = -\phi_n^-(L - x)$. Following the same procedure, we obtain the equation satisfied by the spectrum in this sector as,

$$\frac{e^{-k_b L} - e^{-k_a L}}{1 - e^{-k_a L} e^{-k_b L}} = -\frac{a^{(3)} - a^{(1)}}{a^{(3)} a^{(1)} - 1}. \quad (43)$$

Although the equations (42)-(43) are exact and much simpler compared to Eq. (35), these are not yet exactly solvable for λ in general. However, we earlier mentioned that $\lambda = 0$ and $\lambda = -2\omega$ are eigenvalues of the evolution operator since these satisfy Eq. (35). Here we explicitly find that $\lambda = 0$ satisfies Eq. (43) and therefor belongs to the odd sector (which, as argued earlier, should be discarded for these set of solutions). Whereas $\lambda = -2\omega$ satisfies Eq. (42) and belongs to the even sector. We find analytical expressions for the ‘band’ of eigenvalues close to 0 and -2ω in the large L limit and the corresponding eigenfunctions in the two symmetry sectors. In the following, we demonstrate the results and discuss the relaxation behaviour.

4.1.1 Spectrum in the large- L limit

Eigenvalues near $\lambda = 0$ and relaxation: In the limit of large system size, we expect that the eigenvalues are very close to zero and therefore from Eq. (25), we get,

$$k_a \approx \frac{\sqrt{2\omega D_e}}{D} (= \mu), \quad k_b \approx \sqrt{\lambda/D_e}, \quad (44)$$

The finite value of k_a renders $e^{-k_a L} \approx 0$ in Eqs. (42)-(43). Further, from Eq. (28) one can find that, $a^{(3)} \approx 1$, $a^{(1)} \approx -\frac{1+v/\sqrt{2\omega D_e}}{1-v/\sqrt{2\omega D_e}}$, and the ratio in the rhs of the Eqs. (42)-(43) takes the value, $\frac{a^{(3)}-a^{(1)}}{a^{(3)}a^{(1)}-1} \approx -1$. Consequently, we have, for $o_x = \pm 1$,

$$e^{k_b L} \approx \mp 1 \quad \Rightarrow \quad e^{\sqrt{\frac{\lambda}{D_e}} L} \approx \mp 1 \quad (45)$$

The solutions are,

$$\lambda_n \approx -\frac{(2n-1)^2 \pi^2 D_e}{L^2}, \quad n > 0 \quad (\text{for } o_x = 1), \quad (46a)$$

$$\lambda_{n'} \approx -\frac{(2n')^2 \pi^2 D_e}{L^2}, \quad n' > 0 \quad (\text{for } o_x = -1). \quad (46b)$$

These are the alternate symmetric and antisymmetric bands near $\lambda = 0$. We find that the relaxation rate, that is given by the eigenvalue with real part closest to zero, lies in the symmetric sector and in the large L limit it is given by,

$$|\lambda_1| = \frac{\pi^2 D_e}{L^2}. \quad (47)$$

Alternatively, the relaxation time is, $\tau_L = |\lambda_1|^{-1} = \frac{L^2}{\pi^2 D_e}$. This suggests that, for large systems the relaxation behaviour resembles that of a Brownian particle with an effective diffusion rate D_e . Note that, the solution given in Eq. (46) for the band of eigenvalues are valid as long as $|\lambda_n| \ll 2\omega$, or, $n \ll \sqrt{\tau_L/\tau_t}$, where $\tau_t = (2\omega)^{-1}$ is the relaxation rate of the tumble dynamics.

Correction to the leading behaviour: To evaluate the subleading behaviour we need to keep the first correction terms in λ in Eqs. (42)-(43). Since k_a is finite, in the large L limit we shall neglect $e^{-k_a L}$ and therefore the l.h.s. in both the equations is $e^{-k_b L} \approx e^{-L\sqrt{\lambda/D_e}}$. On the other hand, for small λ , $a^{(3)} \approx 1 - \frac{v}{\omega\sqrt{D_e}}\sqrt{\lambda}$, whereas $a^{(1)} \approx -\frac{1+v/\sqrt{2\omega D_e}}{1-v/\sqrt{2\omega D_e}} + O(\lambda)$. This implies that the corrections in the rhs of Eqs. (42)-(43) are of $O(\sqrt{\lambda})$, and the equations to the first subleading order reads,

$$e^{-L\sqrt{\lambda/D_e}} \approx \mp \left(1 + \frac{v^2}{\omega D_e} \sqrt{\frac{\lambda}{2\omega}} \right), \text{ for } o_x = \pm 1 \text{ respectively.} \quad (48)$$

One can solve the above equation perturbatively by considering $\lambda_n = \lambda_n^{(0)} + \lambda_n^{(1)}$, where $\lambda_n^{(0)} = -\frac{n^2\pi^2 D_e}{L^2}$ are the solution at the leading order in L and $\lambda_n^{(1)} \ll \lambda_n^{(0)}$ are the corrections. We want to find the leading L -dependence of $\lambda_n^{(1)}$. Putting $\lambda_n = \lambda_n^{(0)} + \lambda_n^{(1)}$ in Eq. (48), we get,

$$e^{-L\sqrt{\frac{\lambda_n^{(0)} + \lambda_n^{(1)}}{D_e}}} \approx \mp \left(1 + \frac{v^2}{\omega D_e} \sqrt{\frac{\lambda_n^{(0)} + \lambda_n^{(1)}}{2\omega}} \right). \quad (49)$$

To the first subleading order the left hand side of the Eq. (49) can be written as,

$$e^{-k_b L} \approx e^{-L\sqrt{\frac{\lambda_n^{(0)} + \lambda_n^{(1)}}{D_e}}} = e^{-L\sqrt{\frac{\lambda_n^{(0)}}{D_e}}} \left(1 + \frac{\lambda_n^{(1)}}{\lambda_n^{(0)}} \right)^{1/2} \approx e^{-L\sqrt{\frac{\lambda_n^{(0)}}{D_e}}} e^{-L\sqrt{\frac{\lambda_n^{(0)}}{D_e}}} \left(\frac{\lambda_n^{(1)}}{2\lambda_n^{(0)}} \right) \quad (50)$$

Now, using in the above the expression for $\lambda_n^{(0)}$ from Eq. (46), the l.h.s. of Eq. (49) is obtained as,

$$e^{-k_b L} \approx \mp 1 \times \exp \left(-i \frac{n\pi}{2} \frac{\lambda_n^{(1)}}{\lambda_n^{(0)}} \right) \approx \mp 1 \pm i \frac{n\pi}{2} \frac{\lambda_n^{(1)}}{\lambda_n^{(0)}}, \quad (51)$$

Similarly, we find the right hand side of Eq. (49) to the first subleading order,

$$\mp \left(1 + \frac{v^2}{\omega D_e} \sqrt{\frac{\lambda_n^{(0)} + \lambda_n^{(1)}}{2\omega}} \right) \approx \mp \left(1 + \frac{v^2}{\omega D_e} \sqrt{\frac{\lambda_n^{(0)}}{2\omega}} \right) = \mp 1 \mp i \frac{n\pi}{L} \frac{v^2}{\omega \sqrt{2\omega D_e}}.$$

Then, equating the l.h.s. and r.h.s. of Eq. (49), we get,

$$\lambda_n^{(1)} \approx -\frac{2v^2}{\omega \sqrt{2\omega D_e}} \frac{\lambda_n^{(0)}}{L}, \quad (52)$$

and consequently, the band near $\lambda = 0$ takes the form,

$$\lambda_n = \lambda_n^{(0)} + \lambda_n^{(1)} \approx \lambda_n^{(0)} \left(1 - \frac{2v^2}{\omega \sqrt{2\omega D_e}} \frac{1}{L} \right). \quad (53)$$

Eigenvalues near $\lambda = -2\omega$: We have already mentioned that -2ω is an eigenvalue of the evolution operator that belongs to the symmetric sector. To calculate the band of eigenvalues around it, let us consider $\lambda = -2\omega + \varepsilon$, where ε is presumably small in the large L limit. In this limit,

$$k_a \approx \sqrt{\frac{v^2}{D^2} + \frac{\lambda}{D}}, \quad k_b \approx \sqrt{\varepsilon/D}$$

$$a^{(1)} = 1 - \frac{v^2}{\omega D} - \frac{k_a v}{\omega}, \quad a^{(3)} = -1 - \frac{k_b v}{\omega}.$$

Since $\varepsilon \rightarrow 0$, $a^{(3)} \approx -1$. In the large L -limit, $e^{-k_a L} \rightarrow 0$. Therefore, Eqs (42)-(43) reduce to

$$e^{-k_b L} = \pm 1 \quad \text{for } o_x = \pm 1. \quad (54)$$

The solutions are,

$$\varepsilon_n \approx -\frac{(2n)^2 \pi^2 D}{L^2}, \quad n \geq 0 \quad (\text{for } o_x = 1), \quad (55a)$$

$$\varepsilon_{n'} \approx -\frac{(2n' - 1)^2 \pi^2 D}{L^2}, \quad n' > 0 \quad (\text{for } o_x = -1), \quad (55b)$$

and therefore $\lambda_n = -2\omega + \varepsilon_n$. The corrections to the above expressions can be calculated, which is not shown in the present paper.

4.2 Crossover behaviour of the relaxation time

For passive particles the relaxation time because of diffusion is proportional to L^2/D . RTPs on the other hand also carries a tumble dynamics which relaxes in a timescale $\tau_t \sim (2\omega)^{-1}$. When the system size is very small, the diffusive dynamics relaxes fast and the eigenvalue $\lambda = -2\omega$ corresponding to the tumble dynamics determines the relaxation. However, when the L exceeds the persistent length $L_p \sim v/\omega$, nontrivial system size effects come to play and a crossover to L -dependent relaxation takes place. For $L \gg L_p$, several tumble events occur before reaching the steady state and the relaxation dynamics becomes effectively passive-like, with an activity induced correction as expressed in Eq. (53). This behaviour is shown in Figure 5. We expect this to be a generic feature of active systems, and more generally of processes driven by coloured noise.

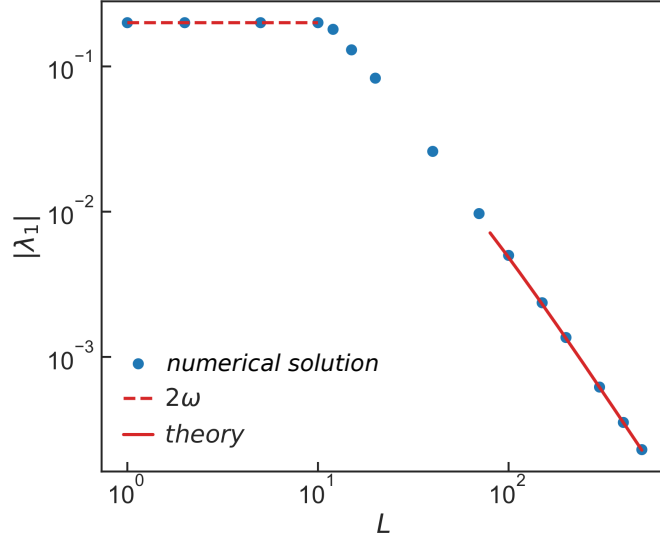


Figure 5: Crossover behaviour of the relaxation rate for different system sizes. Here, $D = 1.0, v = 1.0, \omega = 0.1$. Points are obtained by numerically solving Eq. (42) (symmetric sector) and identifying the solution closest to zero using Mathematica. The crossover to L -dependent relaxation is seen to occur for system sizes very close to $L_p = \frac{v}{\omega} = 10.0$. The large L behaviour is consistent with Eq. (53) for $n = 1$.

4.3 Eigenfunctions and the large-time distribution

Once we have the spectrum, we can completely solve for the coefficients $\alpha_n^i, i = (1, \dots, 4)$. For $o_x = \pm 1$, the coefficients are related as follows:

$$\alpha^{(1)} = -\alpha^{(3)} \frac{a^{(3)} \pm e^{k_b L}}{a^{(1)} \pm e^{k_a L}}, \quad (56)$$

$$\alpha^{(2)} = \pm \alpha^{(1)} a^{(1)} e^{k_a L}, \quad (57)$$

$$\alpha^{(4)} = \pm \alpha^{(3)} a^{(3)} e^{k_b L}, \quad (58)$$

and $\alpha^{(3)}$ is left arbitrary at this point. After incorporating the coefficients in Eq. (29), the expression of the eigenfunctions $|\phi_n(x)\rangle$ becomes,

$$|\phi_n(x)\rangle = \alpha_n^{(3)} \left[\frac{a^{(3)} \pm e^{k_b L}}{a^{(1)} \pm e^{k_a L}} \left(e^{k_a x} \begin{bmatrix} a^{(1)} \\ 1 \end{bmatrix} \pm e^{k_a(L-x)} \begin{bmatrix} 1 \\ a^{(1)} \end{bmatrix} \right) - \left(e^{k_b x} \begin{bmatrix} a^{(3)} \\ 1 \end{bmatrix} \pm e^{k_b(L-x)} \begin{bmatrix} 1 \\ a^{(3)} \end{bmatrix} \right) \right]. \quad (59)$$

The set of equations (56)-(58) can be simplified and the coefficients can be determined

order by order in the large L limit. We shall present results for the band near $\lambda = 0$ and keep the terms which are $\sim O(L^{-1})$.

To this order we find, for $o_x = \pm 1$, $e^{k_b L} \approx \mp(1 - \frac{n\pi}{L} \frac{v^2}{\omega\sqrt{2\omega D_e}})$ using Eqs. (51)-(52), and $\alpha^{(1)} = -\alpha^{(3)} \frac{a^{(3)} \pm e^{k_b L}}{a^{(1)} \pm e^{k_a L}} \approx \mp \alpha^{(3)} [a^{(3)} \pm e^{k_b L}] e^{-k_a L}$. In Eq. (28), keeping the first subleading term in the expression for $a^{(3)}$ and using Eq. (53) to determine $k_b = \sqrt{\lambda/D_e}$ to $O(L^{-1})$, we find, $a^{(3)} \approx 1 - vk_b/\omega \approx 1 - i \frac{v}{\omega} \frac{n\pi}{L}$. Putting these together in Eq. (56) we obtain,

$$\alpha^{(1)} = \pm i \alpha^{(3)} \frac{n\pi}{L} \frac{v}{\omega} \left(1 - \frac{v}{\sqrt{2\omega D_e}}\right) e^{-k_a L}, \text{ for } n = \text{odd/even}. \quad (60)$$

Using the above in Eq. (57) we find,

$$\alpha^{(2)} = i \alpha^{(3)} \frac{n\pi}{L} a^{(1)} \frac{v}{\omega} \left(1 - \frac{v}{\sqrt{2\omega D_e}}\right); \quad (61)$$

and finally, from Eq. (58)

$$\alpha^{(4)} = -\alpha^{(3)} a^{(3)} \left(1 - i \frac{n\pi}{L} \frac{v^2}{\omega\sqrt{2\omega D_e}}\right). \quad (62)$$

Using the coefficients in Eq. (30), we find, at large times $t \gg \omega^{-1}$,

$$\begin{aligned} |P_{\text{tr}}(x, t)\rangle &\approx \sum_{n=1}^{\infty} c_n e^{\lambda_n t} \alpha_n^{(3)} \left(2i \sin \frac{n\pi x}{L} \begin{bmatrix} 1 \\ 1 \end{bmatrix} - i \frac{n\pi v}{\omega L} \cos \frac{n\pi x}{L} \begin{bmatrix} 1 \\ -1 \end{bmatrix} \right. \\ &\quad + \frac{n\pi v}{\omega L} \left\{ \left(1 + \frac{v}{\sqrt{2\omega D_e}}\right) \sin \frac{n\pi x}{L} + i \frac{v}{\sqrt{2\omega D_e}} \left(1 - \frac{2x}{L}\right) \cos \frac{n\pi x}{L} \right\} \begin{bmatrix} 1 \\ 1 \end{bmatrix} \\ &\quad \left. + i \frac{n\pi v}{\omega L} \left(1 - \frac{v}{\sqrt{2\omega D_e}}\right) \left\{ (-1)^{n-1} e^{-k_a(L-x)} \begin{bmatrix} a_n^{(1)} \\ 1 \end{bmatrix} + e^{-k_a x} \begin{bmatrix} 1 \\ a_n^{(1)} \end{bmatrix} \right\} \right), \quad (63) \end{aligned}$$

with $\lambda_n \approx -\frac{n^2\pi^2 D_e}{L^2}$, $n > 0$; here we have used $a_n^{(1)} a_n^{(2)} = 1$. Each term of the summation in Eq. (63) is an eigenfunction evaluated to $O(L^{-1})$. To the *leading order*, each of the eigenfunctions is simply proportional to $\sin \frac{n\pi x}{L}$ and the probability density takes a passive-like form with an effective diffusion constant D_e :

$$\lim_{t \rightarrow \infty} \lim_{L \rightarrow \infty} P(x, t) \approx \sum_{n=1}^{\infty} c_n \alpha_n^{(3)} e^{\lambda_n t} 4i \sin \frac{n\pi x}{L} \equiv P_{\text{passive}}(x, t)|_{D \rightarrow D_e}, \quad (64)$$

while the magnetisation vanishes. In particular, the relaxation mode $n = 1$ is given by $\phi_1(x) \propto \sin \frac{\pi x}{L}$. Note that the *active* contributions in excess to the effective

passivelike contributions, proportional to the active speed v , appear at $O(L^{-1})$ in each term of the distribution $P_{\text{tr}}(x, t) = [1 \ 1] |P_{\text{tr}}(x, t)\rangle$ and magnetization $Q_{\text{tr}}(x, t) = [1 \ -1] |P_{\text{tr}}(x, t)\rangle$. Thus at very large times when only very few n 's contribute, the active part in the distribution and the magnetisation appears only at the subleading order. However, this is not true in the large but intermediate times when all n 's contribute.

To determine the full distribution we need to evaluate the n -dependent constants c_n and $\alpha_n^{(3)}$. Let $\langle\psi_n(x)|$ be the left eigenvector of the evolution operator \mathcal{L} corresponding to eigenvalue λ_n . Then the orthonormality of the $\langle\psi_n(x)|$'s and $|\phi_n(x)\rangle$'s give us $\alpha_n^{(3)}$. The c_n is subsequently determined from the initial condition: $c_n = \int dx \langle\psi_n(x)|P(x, 0)\rangle$. We find the left eigenvectors $\langle\psi_n|$ of \mathcal{L} by noting that it is just the transpose of the right eigenvector of $\mathcal{L}^\dagger \equiv \mathcal{L}|_{\partial_x \rightarrow -\partial_x}$:

$$\begin{aligned} \langle\psi_n(x)| &= |\phi_n(x, -v)\rangle^T \approx \alpha'_n \left(2i \sin \frac{n\pi x}{L} \begin{bmatrix} 1 \\ 1 \end{bmatrix}^T + i \frac{n\pi v}{\omega L} \cos \frac{n\pi x}{L} \begin{bmatrix} 1 \\ -1 \end{bmatrix}^T \right. \\ &\quad - \frac{n\pi v}{\omega L} \left\{ \left(1 - \frac{v}{\sqrt{2\omega D_e}}\right) \sin \frac{n\pi x}{L} - i \frac{v}{\sqrt{2\omega D_e}} \left(1 - \frac{2x}{L}\right) \cos \frac{n\pi x}{L} \right\} \begin{bmatrix} 1 \\ 1 \end{bmatrix}^T \\ &\quad \left. - i \frac{n\pi v}{\omega L} \left(1 + \frac{v}{\sqrt{2\omega D_e}}\right) \left\{ (-1)^{n-1} e^{-k_a(L-x)} \begin{bmatrix} \tilde{a}_n^{(1)} \\ 1 \end{bmatrix}^T + e^{-k_a x} \begin{bmatrix} 1 \\ \tilde{a}_n^{(1)} \end{bmatrix}^T \right\} \right). \end{aligned} \quad (65)$$

$$\Rightarrow \int_0^L dx \langle\psi_n(x)|\phi_m(x)\rangle = -4 \alpha'_n \alpha_n L \left(1 - \frac{i(i + n\pi)v^2}{\omega L \sqrt{2\omega D_e}} \right) \delta_{mn} \quad (66)$$

up to first sub-leading order in L . Invoking the orthonormality condition of the eigenfunctions, we obtain,

$$\alpha'_n \alpha_n \approx -\frac{1}{4L} \left(1 + \frac{i(i + n\pi)v^2}{\omega L \sqrt{2\omega D_e}} \right). \quad (67)$$

Let us consider the initial condition, $|P(x, 0)\rangle = \delta(x - x_0) \begin{bmatrix} s_+ \\ s_- \end{bmatrix}$, s_+, s_- are the probabilities of the initial spin to be plus and minus respectively, and $s_+ + s_- = 1$. Consequently,

$$\begin{aligned}
c_n = \int_0^L dx \langle \psi_n(x) | P(x, 0) \rangle &\approx \alpha'_n \left[2i \sin \frac{n\pi x_0}{L} + \frac{in\pi v}{\omega L} (s_+ - s_-) \cos \frac{n\pi x_0}{L} \right. \\
&- \frac{n\pi v}{\omega L} \left(1 - \frac{v}{\sqrt{2\omega D_e}} \right) \sin \frac{n\pi x_0}{L} + \frac{in\pi v^2}{\omega L \sqrt{2\omega D_e}} \left(1 - \frac{2x_0}{L} \right) \cos \frac{n\pi x_0}{L} \\
&\left. - \frac{in\pi v}{\omega L} \left(1 + \frac{v}{\sqrt{2\omega D_e}} \right) \left\{ (-1)^{n-1} e^{-k_a(L-x_0)} (\tilde{a}_n^{(1)} s_+ + s_-) + e^{-k_a x_0} (s_+ + \tilde{a}_n^{(1)} s_-) \right\} \right].
\end{aligned}$$

Putting c_n 's in Eq. (63) and using Eq. (67), we obtain the form of the state vector after keeping the terms of order $1/L$,

$$\begin{aligned}
|P_{\text{tr}}(x, t)\rangle &= \frac{1}{2L} \sum_{n=1}^{\infty} e^{\lambda_n t} \left(2 \left\{ 1 - \frac{v^2}{L\omega\sqrt{2\omega D_e}} \right\} \sin \frac{n\pi x_0}{L} \sin \frac{n\pi x}{L} \begin{bmatrix} 1 \\ 1 \end{bmatrix} \right. \\
&+ \frac{n\pi v^2}{L\omega\sqrt{2\omega D_e}} \left\{ \left(1 - \frac{2x_0}{L} \right) \cos \frac{n\pi x_0}{L} \sin \frac{n\pi x}{L} + \left(1 - \frac{2x}{L} \right) \cos \frac{n\pi x}{L} \sin \frac{n\pi x_0}{L} \right\} \begin{bmatrix} 1 \\ 1 \end{bmatrix} \\
&- \frac{n\pi v}{L\omega} \left\{ \left(\frac{v}{\sqrt{2\omega D_e}} + m_0 \right) e^{-k_a x_0} - (-1)^n \left(\frac{v}{\sqrt{2\omega D_e}} - m_0 \right) e^{-k_a(L-x_0)} \right\} \sin \frac{n\pi x}{L} \begin{bmatrix} 1 \\ 1 \end{bmatrix} \\
&+ \frac{n\pi v}{L\omega} \left(1 - \frac{v}{\sqrt{2\omega D_e}} \right) \sin \frac{n\pi x_0}{L} \left\{ e^{-k_a x} \begin{bmatrix} 1 \\ a^{(1)} \end{bmatrix} - (-1)^n e^{-k_a(L-x)} \begin{bmatrix} a^{(1)} \\ 1 \end{bmatrix} \right\} \\
&\left. + m_0 \frac{n\pi v}{L\omega} \cos \frac{n\pi x_0}{L} \sin \frac{n\pi x}{L} \begin{bmatrix} 1 \\ 1 \end{bmatrix} - \frac{n\pi v}{L\omega} \sin \frac{n\pi x_0}{L} \cos \frac{n\pi x}{L} \begin{bmatrix} 1 \\ -1 \end{bmatrix} \right). \quad (68)
\end{aligned}$$

Note that, at relaxation time scales ($t \gtrsim L^2/D_e$), only the small n terms ($n = 1, 2$ etc.) survive. Here the dominating contribution comes from the first term of Eq. (68) which is just the effective passive expression, while the nontrivial active contribution occurs in the subleading order. However, at intermediate times $\omega^{-1} \ll t \ll L^2/D_e$, all the n 's contribute and it is not obvious whether the active contributions constitute only a correction to the effective passive behaviour. For this we aim to evaluate the summations in a closed form. Generally, this is not doable for the summations at hand, but we can make certain progress for large values of L using the Poisson summation formula and keeping the leading correction terms in L . We define the following summations that occur in Eq. (68):

$$\begin{aligned}
A(x_1, x_2) &\equiv \sum_{n \geq 1} e^{-D_e t \frac{n^2 \pi^2}{L^2}} \sin \frac{n \pi x_1}{L} \sin \frac{n \pi x_2}{L} \approx \frac{L}{2\sqrt{4\pi D_e t}} \left[e^{-\frac{(x_1-x_2)^2}{4D_e t}} - e^{-\frac{(x_1+x_2)^2}{4D_e t}} - e^{-\frac{(x_1+x_2-2L)^2}{4D_e t}} \right] \\
&= L a_L(x_1, x_2), \\
B(x_1, x_2) &\equiv \sum_{n \geq 1} e^{-D_e t \frac{n^2 \pi^2}{L^2}} \frac{n \pi}{L} \sin \frac{n \pi x_1}{L} \cos \frac{n \pi x_2}{L} \\
&\approx \frac{\pi L}{(4\pi D_e t)^{3/2}} \left[(x_1 + x_2) e^{-\frac{(x_1+x_2)^2}{4D_e t}} + (x_1 - x_2) e^{-\frac{(x_1-x_2)^2}{4D_e t}} + (x_1 + x_2 - 2L) e^{-\frac{(x_1+x_2-2L)^2}{4D_e t}} \right] \\
&= L b_L(x_1, x_2) \\
C(x_1) &\equiv \sum_{n \geq 1} e^{-D_e t \frac{n^2 \pi^2}{L^2}} \frac{n \pi}{L} \sin \frac{n \pi x_1}{L} \approx \frac{\pi L}{2(4\pi D_e t)^{3/2}} \left[x_1 e^{-\frac{x_1^2}{4D_e t}} + (x_1 - 2L) e^{-\frac{(x_1-2L)^2}{4D_e t}} \right] \\
&= L c_L(x_1)
\end{aligned} \tag{69}$$

The terms in Eq. (68) that involve $(-1)^n$ are just $C(L - x_1)$, since,

$$C(L - x_1) = - \sum_{n \geq 1} (-1)^n e^{-D_e t \frac{n^2 \pi^2}{L^2}} \frac{n \pi}{L} \sin \frac{n \pi x_1}{L}.$$

The L -dependent terms that are kept in the final (Gaussian-like) expressions in Eq. (69) are chosen in view of the symmetries satisfied by the discrete summation, that are reflected in the symmetries of the density and magnetisation profile:

$$\begin{aligned}
P(x, t; x_0, m_0) &= P(L - x, t; L - x_0, -m_0), \\
Q(x, t; x_0, m_0) &= -Q(L - x, t; L - x_0, -m_0).
\end{aligned} \tag{70}$$

Now we rewrite Eq. (68) in terms of a_L , b_L and c_L ,

$$\begin{aligned}
|P_{\text{tr}}(x, t)\rangle &\approx \frac{1}{2} \left(2 a_L(x_0, x) \begin{bmatrix} 1 \\ 1 \end{bmatrix} + m_0 \frac{v}{\omega} b_L(x, x_0) \begin{bmatrix} 1 \\ 1 \end{bmatrix} - \frac{v}{\omega} b_L(x_0, x) \begin{bmatrix} 1 \\ -1 \end{bmatrix} \right. \\
&+ \frac{v^2}{\omega \sqrt{2\omega D_e}} \left\{ \left(1 - \frac{2x_0}{L}\right) b_L(x, x_0) + \left(1 - \frac{2x}{L}\right) b_L(x_0, x) \right\} \begin{bmatrix} 1 \\ 1 \end{bmatrix} \\
&- \frac{v}{\omega} \left\{ \left(\frac{v}{\sqrt{2\omega D_e}} + m_0\right) e^{-k_a x_0} c_L(x) + \left(\frac{v}{\sqrt{2\omega D_e}} - m_0\right) e^{-k_a(L-x_0)} c_L(L-x) \right\} \begin{bmatrix} 1 \\ 1 \end{bmatrix} \\
&\left. + \frac{v}{\omega} \left(1 - \frac{v}{\sqrt{2\omega D_e}}\right) \left\{ e^{-k_a x} c_L(x_0) \begin{bmatrix} 1 \\ a^{(1)} \end{bmatrix} + e^{-k_a(L-x)} c_L(L-x_0) \begin{bmatrix} a^{(1)} \\ 1 \end{bmatrix} \right\} \right), \tag{71}
\end{aligned}$$

which gives an approximate closed form expression of the state vector in the large L limit in terms of known functions. It is now evident that the ‘active’ contributions do appear at the leading order only.

4.4 Semi-infinite line with absorbing barrier at $x = 0$:

The symmetries are no longer present in the semi-infinite geometry and the state vector at large times can be obtained by taking the limit $L \gg x, x_0$ in Eq. (71):

$$\begin{aligned}
|P_{\text{tr}}^\infty(x, t)\rangle &= \frac{1}{2} \left(\frac{1}{\sqrt{4\pi D_e t}} \left\{ e^{-\frac{(x-x_0)^2}{4D_e t}} - e^{-\frac{(x+x_0)^2}{4D_e t}} \right\} \begin{bmatrix} 1 \\ 1 \end{bmatrix} \right. \\
&\quad + \frac{m_0 v}{\omega} \frac{\pi}{(4\pi D_e t)^{3/2}} \left\{ (x-x_0) e^{-\frac{(x-x_0)^2}{4D_e t}} + (x+x_0) e^{-\frac{(x+x_0)^2}{4D_e t}} \right\} \begin{bmatrix} 1 \\ 1 \end{bmatrix} \\
&\quad + \frac{v}{\omega} \frac{2\pi}{(4\pi D_e t)^{3/2}} \left\{ \frac{v}{\sqrt{2\omega D_e}} (x+x_0) e^{-\frac{(x+x_0)^2}{4D_e t}} - \left(\frac{v}{\sqrt{2\omega D_e}} + m_0 \right) x e^{-k_a x_0} e^{-\frac{x^2}{4D_e t}} \right\} \begin{bmatrix} 1 \\ 1 \end{bmatrix} \\
&\quad + \frac{v}{\omega} \left(1 - \frac{v}{\sqrt{2\omega D_e}} \right) \frac{2\pi}{(4\pi D_e t)^{3/2}} x_0 e^{-k_a x} e^{-\frac{x_0^2}{4D_e t}} \begin{bmatrix} 1 \\ a^{(1)} \end{bmatrix} \\
&\quad \left. + \frac{v}{\omega} \frac{\pi}{(4\pi D_e t)^{3/2}} \left\{ (x-x_0) e^{-\frac{(x-x_0)^2}{4D_e t}} - (x+x_0) e^{-\frac{(x+x_0)^2}{4D_e t}} \right\} \begin{bmatrix} 1 \\ -1 \end{bmatrix} \right). \tag{72}
\end{aligned}$$

All the terms in the above expression are $\sim O(t^{-3/2})$, and therefore ‘passive’ as well as the ‘active’ contributions are equally important in determining the large time behaviour in the semi infinite domain. From Eq. (72) we find the distribution and magnetisation profile by respectively adding and subtracting the rows:

$$\begin{aligned}
P_{\text{tr}}^\infty(x, t) &= \frac{1}{\sqrt{4\pi D_e t}} \left\{ e^{-\frac{(x-x_0)^2}{4D_e t}} - e^{-\frac{(x+x_0)^2}{4D_e t}} \right\} \\
&\quad + \frac{v^2}{\omega \sqrt{2\omega D_e}} \frac{2\pi}{(4\pi D_e t)^{3/2}} (x+x_0) e^{-\frac{(x+x_0)^2}{4D_e t}} \\
&\quad + \frac{m_0 v}{\omega} \frac{\pi}{(4\pi D_e t)^{3/2}} \left\{ (x-x_0) e^{-\frac{(x-x_0)^2}{4D_e t}} + (x+x_0) e^{-\frac{(x+x_0)^2}{4D_e t}} \right\} \\
&\quad - \frac{v}{\omega} \frac{2\pi}{(4\pi D_e t)^{3/2}} \left\{ \left(\frac{v}{\sqrt{2\omega D_e}} + m_0 \right) x e^{-k_a x_0} e^{-\frac{x^2}{4D_e t}} + \frac{v}{\sqrt{2\omega D_e}} x_0 e^{-k_a x} e^{-\frac{x_0^2}{4D_e t}} \right\}, \tag{73}
\end{aligned}$$

and,

$$\begin{aligned}
Q_{\text{tr}}^\infty(x, t) &= \frac{v}{\omega} \frac{\pi}{(4\pi D_e t)^{3/2}} \left\{ (x-x_0) e^{-\frac{(x-x_0)^2}{4D_e t}} - (x+x_0) e^{-\frac{(x+x_0)^2}{4D_e t}} \right\} \\
&\quad + \frac{v}{\omega} \frac{2\pi}{(4\pi D_e t)^{3/2}} x_0 e^{-k_a x} e^{-\frac{x_0^2}{4D_e t}}. \tag{74}
\end{aligned}$$

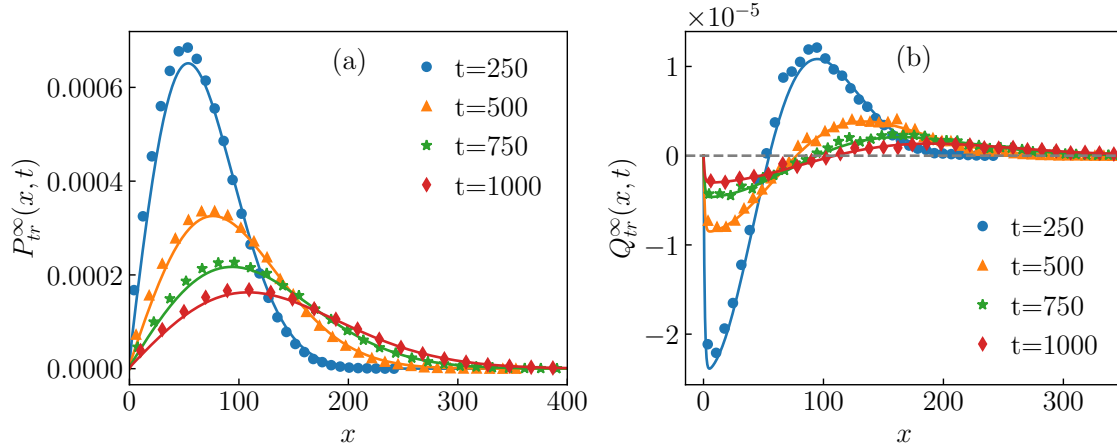


Figure 6: (a) Probability density at different times. Solid lines are the theoretical expression (Eq. (73)). (b) The magnetisation profile at different times. Solid lines are from the expression in Eq. (74). Here $x_0 = 1$, $m_0 = 0$, $\omega = 0.1$, $v = 1$, $D = 1$.

The profiles carry an interesting structure. In each of Eqs. (73)-(74), the last term falls exponentially in distance and is the ‘kinetic boundary layer’ with a ‘skin depth’ k_a^{-1} , while the other terms form the ‘scaling’ part of the profile. In Eq. (73) the last but one term falls rapidly if the initial position exceeds the skin depth.

In Eq. (73) we can immediately identify the *passive* and *active* contributions to the distribution. It is useful to look at the relative magnitude of these two contributions. We first note that, at space-time scales such that $t \gg \{\frac{x_0^2}{D_e}, \frac{x^2}{D_e}\}$, $P_{\text{passive}}^{\infty}(x, t) = \frac{1}{\sqrt{4\pi D_e t}} \{e^{-\frac{(x-x_0)^2}{4D_e t}} - e^{-\frac{(x+x_0)^2}{4D_e t}}\} \approx \frac{x x_0}{2\sqrt{\pi} (D_e t)^{3/2}}$ and from Eq. (73), $P_{\text{active}}^{\infty} = P_{\text{tr}}^{\infty} - P_{\text{passive}}^{\infty} \sim O(t^{-3/2})$, i.e. both occur at the same order. The relative weight of active and passive contributions is,

$$\tilde{R}(x_0, x) = \lim_{t \gg \frac{x_0^2}{D_e}, \frac{x^2}{D_e}} \frac{P_{\text{active}}^{\infty}}{P_{\text{passive}}^{\infty}} = \frac{v}{2\omega} \left[\left(m_0 + \frac{v}{\sqrt{2\omega D_e}} \right) \frac{1 - e^{-k_a x_0}}{x_0} + \frac{v}{\sqrt{2\omega D_e}} \frac{1 - e^{-k_a x}}{x} \right], \quad (75)$$

which is finite throughout the system for any finite x_0 , and can actually attain dominant role for highly persistent (small ω or large v) run and tumble motion. The effect of activity becomes more prominent when the particle is in the ‘boundary layer’ $x \lesssim k_a^{-1}$. Beyond that this part decays slowly as x^{-1} , and asymptotically the contribution from initial position x_0 only remains. In fact, it can be shown from Eq. (73) that, when both x and t is very large such that $u = x/\sqrt{D_e t}$ is finite, both the

active and passive contributions are $\sim (D_e t)^{-1}$, and their ratio becomes,

$$R(x_0) = \lim_{\{x,t \rightarrow \infty, \frac{x}{\sqrt{D_e t}} = u\}} \frac{P_{\text{active}}^\infty}{P_{\text{passive}}^\infty} = \frac{v}{2\omega} \left(m_0 + \frac{v}{\sqrt{2\omega D_e}} \right) \frac{1 - e^{-k_a x_0}}{x_0}. \quad (76)$$

The impact of the active contribution can be understood by considering the case of

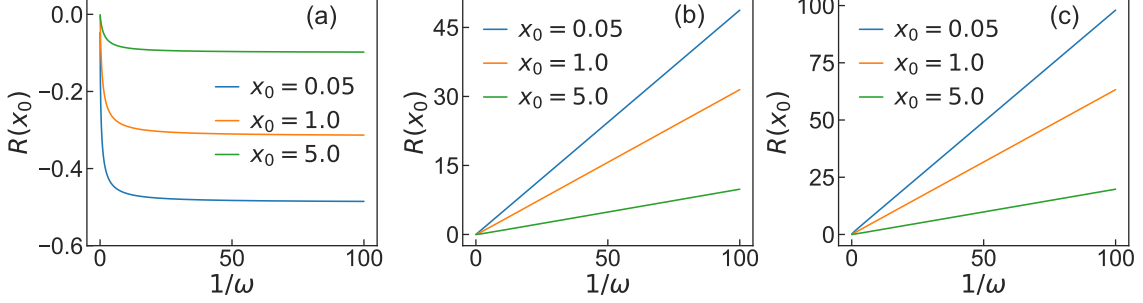


Figure 7: $R(x_0)$ from Eq. (76) as a function of $1/\omega$ for (a) $m_0 = -1$, (b) $m_0 = 0$, (c) $m_0 = 1$ for different values of x_0 . Here $v = D = 1$.

a highly persistent (small ω) particle, starting at some $x_0 \lesssim k_a^{-1} = \frac{D}{\sqrt{2\omega D_e}}$ (which is not necessarily small). In this case $R(x_0) \approx \frac{v}{2\omega} \left(m_0 + \frac{v}{\sqrt{2\omega D_e}} \right) k_a \approx \frac{v^2}{\omega D} s_+ - \frac{1}{2}$: when there is a finite probability of the initial spin to be positive, the active to passive ratio is very high and the distribution is almost completely dominated by the active part for all x . In the extreme case where $s_+ = 0$ and the particles always start with a negative spin, the ratio $R \approx -\frac{1}{2}$, implying that the distribution at larger x values will be diminished to the half of what would otherwise be expected for an entirely effective passive scenario. The nature of $R(x_0)$ is shown in Figure 7.

4.4.1 Discussion: thermal noise and the late time behaviour of active particles

This everlasting and often dominant influence of activity to the distribution is partly related to the initial penetration of the particles before they start tumbling. But that effect is strongly modulated in the presence of thermal noise. The nontrivial effect of diffusion is reflected in the flux at $x = 0$:

$$\begin{aligned} J(0, t) &= \left[-D \frac{\partial P(x, t)}{\partial x} + v Q(x, t) \right]_{x=0} \\ &= -\frac{1}{2\sqrt{\pi}(D_e t)^{\frac{3}{2}}} \left[D_e x_0 + \frac{Dv}{2\omega} \left(m_0 + \frac{v}{\sqrt{2\omega D_e}} \right) (1 - e^{-k_a x_0}) \right]. \quad (77) \end{aligned}$$

For $D = 0$, the terms in the square bracket reduce to $D_e x_0$, similar to passive particles; and this flux is due to the particles with instantaneous negative spin. For nonzero but small D , $e^{-k_a x_0}$ is still negligible and the flux gains a contribution that couples thermal noise and activity: $\frac{Dv}{2\omega}(m_0 + 1 - \frac{\omega D}{v^2}) = D(\frac{v}{\omega}s_+ - \frac{D}{2v})$. If $s_+ > 0$ the change is proportional to $\frac{Dv}{\omega}$, which is positive. This shows that the particles with *initial positive spin* largely contribute to an additional flux at the origin. This is consistent with the picture that at short times the particles with initial positive spin move away from the origin, which makes them available in the system to contribute to the noise driven flux at late times. There is also a spin-independent reduction of the flux amounting to $-\frac{D^2}{2v}$, which is much smaller but pertains to the diffusive spread $\sim O(\frac{D}{v})$ over the persistent motion. This indicates a complex nonlinear effect of diffusion on the behaviour of active particle dynamics, which becomes prominent when D is finite.

The magnetisation also gives important insights to the dynamics at large times. As expected, $Q_{\text{tr}}(x, t)$ vanishes in the passive case ($v = 0$). It is interesting to note that the magnetisation profile in Eq. (74) is independent of the initial magnetisation m_0 , although the probability density strongly depends on it. At large times the total magnetisation in the system is given by,

$$Q^\infty(t) = \int_0^\infty Q_{\text{tr}}^\infty(x, t) dx = \frac{v D}{\omega \sqrt{2\omega D_e}} \frac{2\pi}{(4\pi D_e t)^{3/2}} x_0 e^{-\frac{x_0^2}{4D_e t}}, \quad (78)$$

which is positive at all times and undergoes a slow algebraic decay. It is tempting to relate this result to the simple fact that the particles with negative spin are more prone to go out of the absorbing boundary at $x = 0$. However, we need to take a closer look at this point. Quite remarkably, in the absence of thermal diffusion ($D = 0$), $Q^\infty(t)$ vanishes, implying that there are equal numbers of positive and negative spin particles in the system. As shown in the Figure 8, the ‘pure active ($D = 0$)’ part of the magnetisation is positive at larger x values; as we reduce x beyond some point it becomes negative and monotonically decreasing to its minimum at $x = 0$ signifying a discontinuity at the absorbing end. Further from Eqs. (73)-(74), $Q_{\text{tr}}(0, t) = -P_{\text{tr}}(0, t)$ for $D = 0$, which implies that only the negative spin particles cross the origin, leading to the condition $P^+(0, t) = 0$. These corroborates the general prevalence of negative spin particles near the origin before these are eventually absorbed. Yet, the net balance of positive and negative spin particles is maintained in the system.

The picture is considerably revised in the presence of even a small thermal diffusion. For very small x the time to hit the absorbing boundary is small. But at such small

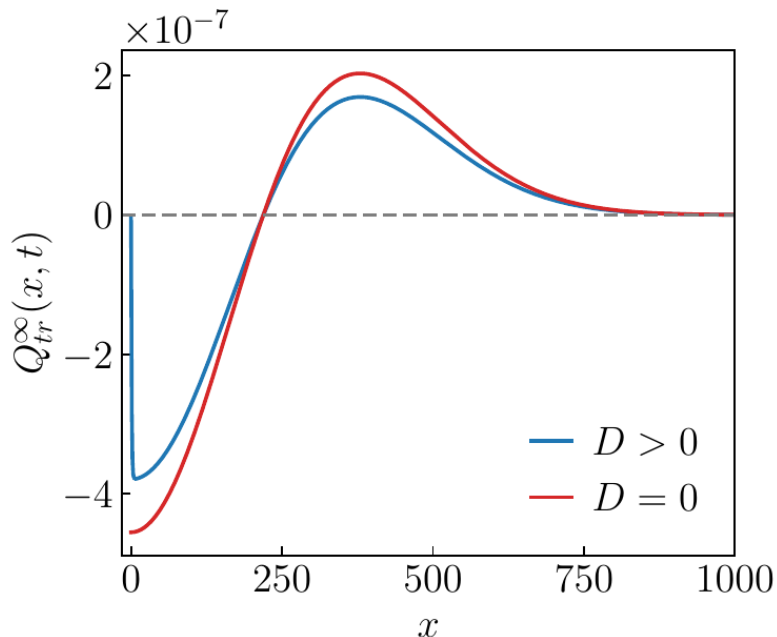


Figure 8: Comparison of magnetisation density using Eq. (74) for $D > 0$ and $D = 0$ cases. Here $v = 1$ and $x_0 = 1$. We have taken $\{D = 1, \omega = 0.1\}$, and $\{D = 0, \omega = 1/12\}$ such that both cases are activity dominated and the effective diffusivities are also the same ($D_e = 6$).

times diffusion dominates over drift, and therefore it compels a larger fraction of the particles near $x = 0$ to get absorbed. However the region near $x = 0$ is majorly populated by the negative spin particles, implying their enhanced elimination from the system because of the diffusion induced absorption, which leads to an imbalance of the two species of particles. In this way the discontinuity at the boundary is also removed through the formation of the ‘kinetic boundary layer’, which in this case is a depletion layer, of width $k_a^{-1} \sim D/v$ for small D .

5 Universality in the large time distribution

The density profile for underdamped passive Brownian motion in one dimension with absorbing barrier at $x = 0$ closely resembles the distribution in Eq. (73) for RTP, except that in the former case the boundary layer structure is richer and a boundary discontinuity is present. The solution for the underdamped case is complicated and originally given in the Laplace space w.r.t. time [47]. However it is relatively simpler

to extract the approximate large time behaviour, which is shown in the Appendix B. Note that the underdamped passive problem is exactly equivalent to the absorbing boundary problem of active Ornstein-Uhlenbeck process (AOUP) in the absence of translational noise and external forces, and so are the solutions. The striking resemblance of such disparate processes, one of which is a passive process, with the only common point being the presence of an additive exponentially correlated noise evokes a general form for the large time distribution in presence of an absorbing barrier,

$$\begin{aligned}
P_{\text{tr}}^{\infty}(x, t; x_0) &= \frac{1}{\sqrt{4\pi D_e t}} \left\{ e^{-\frac{(x-x_0)^2}{4D_e t}} - e^{-\frac{(x+x_0)^2}{4D_e t}} \right\} \\
&+ \frac{l_M}{2\sqrt{\pi} (D_e t)^{3/2}} (x+x_0) e^{-\frac{(x+x_0)^2}{4D_e t}} \\
&+ \frac{u_0 \tau_p}{4\sqrt{\pi} (D_e t)^{3/2}} \left\{ (x-x_0) e^{-\frac{(x-x_0)^2}{4D_e t}} + (x+x_0) e^{-\frac{(x+x_0)^2}{4D_e t}} \right\} \\
&+ \text{Boundary layer}, \tag{79}
\end{aligned}$$

where u_0 is the average initial velocity, τ_p is the noise correlation time or persistence time, and l_M is the Milne length [48]. Clearly, the distribution has three components, $P_{\text{tr}}^{\infty}(x, t) = P_{\text{BM}} + P_{\text{CS}} + P_{\text{BL}}$, where P_{BM} is the passive-like contribution with an effective diffusivity, P_{BL} is the dynamics dependent boundary layer, and P_{CS} is proposed as the *universal scaling form* emergent due to the coloured noise, $P_{\text{CS}}(x, t; x_0) = \frac{l_M}{D_e t} \psi\left(\frac{x}{\sqrt{D_e t}}; \frac{x_0}{\sqrt{D_e t}}\right)$ with,

$$\psi(y; y_0) = \frac{u_0 \tau_p / l_M}{4\sqrt{\pi}} \left\{ (y-y_0) e^{-\frac{(y-y_0)^2}{4}} + (y+y_0) e^{-\frac{(y+y_0)^2}{4}} \right\} + \frac{y+y_0}{2\sqrt{\pi}} e^{-\frac{(y+y_0)^2}{4}}. \tag{80}$$

The scaling function, however, depends on a parameter $\frac{u_0 \tau_p}{l_M}$ that takes different values for different initial conditions and noise realisations. For RTP, $u_0 = m_0 v$, $\tau_p = (2\omega)^{-1}$, and $l_M = \frac{v}{\sqrt{2\omega D_e}} l_p$ where $l_p = \frac{v}{2\omega}$ is the persistent length scale. For the nonthermal ($D = 0$) RTP, $l_M = l_p$, the boundary layer vanishes, and a boundary discontinuity is created. Note that l_M changes in an interesting manner in the presence of diffusion. For the underdamped passive motion, $D_e = D$, $\tau_p = \frac{m}{\gamma}$ and $l_M \approx 1.46 l_p$ with $l_p = \sqrt{D \tau_p}$, where m is the mass, γ is the damping coefficient, and D is the thermal diffusivity. For initial conditions such that $u_0 = 0$, the scaling function does become universal. Using simulations we have checked the validity of Eqs. (79)-(80) for nonthermal ABP as well, which is shown in the Appendix C.

6 Concluding remarks

Analytical results discussed in this paper provide a number of insights for nonequilibrium boundary driven systems subject to an exponentially correlated noise. We found that the complex interplay of overdamped run and tumble motion and thermal noise gives rise to a boundary layer as well as a finite bulk magnetisation, both marking significant departure from an overdamped passive physics. For zero boundary magnetisation the steady state current is still proportional to the density difference at the boundaries, while the proportionality constant is a nontrivial function of the system size. Notably, in the large L limit, although the bulk density profile and current goes over to the usual diffusive behaviour, both L and x carry an important correction of the order of the Milne length: $x \rightarrow x + l_M$ and $L \rightarrow L + 2l_M$, reminiscent of an effective absorbing condition outside the boundaries. The fact that the bulk density profile is close to that of a passive particle is related to the finiteness of the temporal correlation of the persistent dynamics. A Seebeck-like effect is observed for nonzero boundary magnetisation. In the equilibrium Seebeck effect, the particles carry charge as well as velocity, the latter being distributed according to the two temperatures at the boundaries. It is plausible that whenever the particles carry more than one attributes, as in the underdamped as well as the active cases, such effects might occur. An intriguing question is whether magnetisation, which doesn't have any passive counterpart nor has an associated flux, may still be regarded as a thermodynamic force.

In regard to the dynamics, the boundary value problem reduces to a problem with absorbing boundaries at both ends. This allows us to find the spectrum using a reflection symmetry. For large L , the eigenvalues and eigenfunctions of the time evolution operator have been found exactly and the full initial value problem is solved at large times $t \gg \omega^{-1}$. The spectrum is arranged in two distinct bands, one around $\lambda = 0$ which determines the long time behaviour, and the other around $\lambda = -2\omega$. The relaxation rate shows an interesting crossover, being a constant for small systems and L -dependent for large systems, which takes a passive-like form in the thermodynamic limit. Further, at large but intermediate times ($\omega^{-1} \ll t \ll L^2/D_e$) the distribution carries strong and often dominant *intrinsically active* signatures not captured by any effective passive description. This behaviour is carried over to the semi-infinite limit, where the density and magnetisation profiles consist of a boundary layer at the absorbing end and an activity dominated scaling regime in the bulk. These features are also present in many other systems e.g. the underdamped passive case, the AOUP, and the ABP, where the main quantitative difference occurs in the detailed structure of the boundary layer and the Milne length.

The striking similarity of the distribution for active and underdamped passive dynamics in the boundary driven problem points to a new universality in the physics induced by exponentially correlated noises. The unconstrained motions of active and the underdamped passive particles simply go over to a diffusive dynamics at large times, as a consequence of the central limit theorem. The active and passive processes are however very different in the presence of interaction, and a set of model independent features for active single-file dynamics were found recently [49]. Contrary to both of the above, in the absorbing boundary problem the proposed universal distribution in Eq. (79) is new and different from the diffusive one, and also it appears to hold for any exponentially correlated noise *including* the underdamped passive motion. We further expect that the steady state of the boundary driven active and underdamped passive problem will have a structure similar to Eq. (7), i.e. sum of a linear profile and boundary layers [42, 43]. We must however be cautious that such similarities might be broken in presence of trapping and other forces, other noises, or interactions.² This is primarily because the active motion that we are considering is overdamped, which is different from the underdamped motion in general. For that matter, it would be worthwhile to look into the interplay of underdamped motion and coloured noise, e.g. by comparing the behaviour of underdamped and overdamped active dynamics under similar external conditions.

Keeping the differences in mind, it seems plausible that the formation of a boundary layer in presence of absorbing boundary is generic for motions driven by coloured noise. We however emphasize the importance of continuous values of the noise, specifically for the athermal case. The one dimensional athermal AOUP gives rise to boundary layers as well as a boundary discontinuity, while the athermal RTP results in a boundary discontinuity only which is smoothed to a boundary layer in presence of thermal noise. For the RTP in a 1D box with reflecting boundaries a delta peak occurs at the walls that is converted to an exponential boundary layer for $D > 0$ [13]. On the other hand, in 2-dimension where the orientation of RTP takes continuous values, a boundary layer is reported for reflecting boundaries even in the absence of thermal noise [51], and we would expect such boundary layers for absorbing boundary as well. Studying absorbing boundary problems with other realisations of continuous valued coloured noise would be useful in this regard.

Apart from the boundary layer which is dynamics dependent, it is instructive to investigate the extent of validity of the proposed universality of the late time density profile in Eqs. (79)-(80), in particular for the underdamped active processes.

²For example a trapped athermal AOUP has a very different steady state compared to a trapped underdamped passive particle [50].

Further, which of the emergent features are affected in presence of an additional translational noise is a relevant question. It appears reasonable to speculate that the structure of the density profile will remain the same; however the additional length scale introduced because of the thermal noise would nontrivially change the Milne length, and will also alter the boundary layer and particle demography so as to remove the boundary discontinuity present in the nonthermal cases.

In conclusion, we believe that this work will be useful for the future studies of boundary driven active processes. It strives to elucidate the interplay of thermal noise with activity, and in particular points to a novel universality for the motion involving coloured noise. A detailed and more general understanding of the distribution in Eqs. (79)-(80) will be important in gaining insights into the nature of such processes. Whether these features survive when the noise correlation is non-exponential yet short ranged, as well as the qualitative changes introduced by interactions, will be of particular interest.

Acknowledgments: AD acknowledges discussions with Soumyadip Banerjee.

Appendices

A. Exit probability of RTP at the left boundary:

The exit probabilities $E_{\pm}(x)$ for an RTP is obtained by solving two coupled backward equations with boundary conditions, $E_{\pm}(0) = 1, E_{\pm}(L) = 0$ (see Eq. (51) of [13] with signs interchanged). The equations suggest that $E_{\pm}(x)$ is linearly related to $P_{\mp}(x)$, and their differences coming from the different boundary values can simply be taken care of by the following substitutions,

$$P_+(x) = (P_0^+ - P_1^+) E_-(x) + P_1^+, \quad (81a)$$

$$P_-(x) = (P_0^- - P_1^-) E_+(x) + P_1^-. \quad (81b)$$

The above can be combined for the density and magnetisation profile, which takes a particularly simple form for zero boundary magnetisations,

$$P(x) = P_1 - \Delta P [E_+(x) + E_-(x)], \quad Q(x) = \Delta P [E_+(x) - E_-(x)], \quad (82)$$

where $\Delta P = P_1 - P_0$. This relation is used for simulating the steady state distributions. Note that the results for E_{\pm} reported in Eqs. (C5) of [13] carry some typo.

The correct result is,

$$E_m(x) = \frac{(1 + e^{-\mu L})x - \frac{v}{2\omega}(m - \frac{v}{\mu D})[1 - e^{-\mu x}] + \frac{v}{2\omega}(m + \frac{v}{\mu D})[e^{-\mu(L-x)} - e^{-\mu L}]}{L(1 + e^{-\mu L}) + \frac{v^2}{\omega\mu D}(1 - e^{-\mu L})}. \quad (83)$$

Using $m = \pm 1$ one can find the expressions for E_{\pm} .

B. Large time distribution of a passive underdamped Brownian motion in presence of an absorbing barrier:

The absorbing boundary problem of a one dimensional underdamped Brownian motion is surprisingly challenging. The problem was posed in 1945 [52] and finally solved after four decades [47, 53]. Here we are interested in the late time behaviour of the distribution of position of the unbiased underdamped motion. The full solution is quite complex and is originally given in the Laplace space (s) w.r.t. time (Eq. (4.4) of [47]):

$$\begin{aligned} \tilde{P}_{x_0, v_0}(x, v; s) &= \frac{e^{-v^2/2}}{\sqrt{8\pi}} \sum_{n=0}^{\infty} \frac{e^{-q_n|x-x_0|}}{q_n} f_n^{\mp}(v) f_n^{\mp}(v_0) \\ &\quad - \frac{e^{-v^2/2}}{\sqrt{32\pi}} \sum_{m,n=0}^{\infty} \frac{\sigma_{mn}}{q_m q_n} e^{-q_m x - q_n x_0} f_m^+(v) f_n^-(v_0), \quad \mp \text{ is for } x \lesseqgtr x_0, \end{aligned} \quad (84)$$

where $q_n = \sqrt{n+s}$, $\sigma_{mn} = \frac{1}{q_m+q_n} \frac{1}{Q_m Q_n} = \sigma_{nm}$ with $Q_n = \lim_{N \rightarrow \infty} \frac{\sqrt{n!N!} \exp(2q_n \sqrt{N+1})}{\prod_{r=0}^{N+n} (q_r + q_n)}$, and $f_n^+(v) = f_n(v) = \frac{e^{v^2/4}}{\sqrt{n!}} \left[(-1)^n e^{z^2/4} \frac{d^n}{dz^n} e^{-z^2/2} \right]_{z=2q_n-v}$, $f_n^-(v) = f_n(-v)$. Here all the variables are non-dimensionalised, $t \rightarrow t\gamma/m$, $x \rightarrow x\sqrt{\gamma/(mD)}$, $v \rightarrow v\sqrt{m/(D\gamma)}$, m is the mass of the particle. To find the distribution at large times we need to extract the leading behaviour of \tilde{P} in the $s \rightarrow 0$ limit. In this limit, the summations with only $m = 0$ or $n = 0$ will contribute in Eq. (84), and the different quantities are evaluated as,

- I. $f_0(v) \approx e^{-s+v\sqrt{s}}$, $f_n(v) \approx \frac{\Phi_n(v)}{\sqrt{n!}} e^{-n+v\sqrt{n}}$ for $n > 0$, where $\Phi_n(v)$ is a polynomial of degree n .
- II. The Q_n 's are evaluated using Euler-Maclaurin formula: $\sum_{r=1}^N f(r) = \int_1^N f(x)dx + \frac{f(1)+f(N)}{2} + \mathcal{R}_N$, where \mathcal{R}_N is the residue. Without considering \mathcal{R}_N we find, $Q_0 \approx \frac{1}{2\sqrt{s}} e^{\frac{3}{2}\sqrt{s}}$, $Q_n(s) \approx \left[\frac{n!}{n(1+\sqrt{n})} \right]^{\frac{1}{2}} e^{\frac{n}{2}+\sqrt{n}} e^{-\sqrt{s/n}}$ for $n > 0$. If we take the

residue term into account, the exponent $\frac{3}{2}$ in $Q_0(s)$ would be slightly modified; e.g. the first correction would give an exponent $\frac{3}{2} - \frac{1}{24} \approx 1.458$. In Q_n , the residue would introduce a slowly varying prefactor $b_n : Q_n \rightarrow b_n Q_n$.

Putting these together, and integrating out the velocity, we find the distribution of the particle's position in the Laplace space,

$$\tilde{P}_{x_0, v_0}(x; s) \approx \frac{e^{-\frac{3}{2}s}}{2\sqrt{s}} \left[e^{-(|x-x_0|\pm v_0)\sqrt{s}} - e^{-(x+x_0+2l_M+v_0)\sqrt{s}} \right] + \tilde{P}_{BL}(x; s), \quad (85)$$

where $l_M \approx 1.458$, \pm is for $x \lesseqgtr x_0$, and the boundary layer profile is given by,

$$\begin{aligned} \tilde{P}_{BL}(x; s) \approx & \frac{1}{2} \sum_{n=0}^{\infty} \left[\frac{1 + \sqrt{n}}{n} \right]^{\frac{1}{2}} \frac{e^{-\frac{3}{2}n - \sqrt{n}}}{n! b_n} e^{-(v_0 - \frac{1}{\sqrt{n}})\sqrt{s}} \\ & \times \left[H(n) e^{-x\sqrt{n}} e^{-(x_0+v_0)\sqrt{s}} + \Phi_n(-v_0) e^{-(x_0-v_0)\sqrt{n}} e^{-x\sqrt{s}} \right], \quad (86) \end{aligned}$$

with $H(n) = \frac{1}{\sqrt{2\pi}} \int_{-\infty}^{\infty} dv \Phi_n(v) e^{-\frac{v^2}{2} + v\sqrt{n}}$. Plugging in the units and taking the inverse transform, we find the leading time dependence of the density profile for the problem, which is given by Eq. (79).

The distribution is markedly different from that obtained in the usual overdamped problem. It contains a rich 'kinetic boundary layer' structure of a finite skin depth $\sim l_p = \sqrt{mD/\gamma}$ near the absorbing walls. Secondly, far from the wall at large times the distribution takes a scaling-like form $P_{sc} = P_{x_0, v_0}^{\infty}(x, t) - P_{BL}$ which corresponds to a spatial shift $x \rightarrow x + l_M$. P_{sc} satisfies the absorbing condition at $x = -l_M$ instead of $x = 0$ [54], i.e. $P_{sc}(-l_M, t) = 0$, implying that l_M is the Milne length. In [53] the Milne length is exactly determined, $l_M = -\zeta(\frac{1}{2}) l_p \approx 1.460 l_p$, a value approximated remarkably well by the Euler-Maclaurin formula. Also note the factor $e^{-\frac{3}{2}s}$ in Eq. (85) that corresponds to a temporal shift, $t \rightarrow t - \frac{3}{2}\tau_p$ with $\tau_p = m/\gamma$, suggesting that P_{sc} pertains to an initial condition at $t = \frac{3}{2}\tau_p$ instead of $t = 0$ [54].

C. Distribution of ABPs on a semi-infinite line in presence of absorbing boundary:

The equation of motion of an overdamped ABP is given by,

$$\dot{x} = v \cos \theta(t) + \eta(t), \quad \dot{\theta} = \sqrt{2D_r} \zeta(t), \quad (87)$$

where v is the self-propulsion speed, θ is the instantaneous orientation of the particle which takes on continuous values, and η is the thermal noise; here θ evolves as

a Brownian particle with (rotational) diffusivity D_r . Since $\langle \cos(\theta(t)) \cos(\theta(t')) \rangle = e^{-D_r |t-t'|}$, the dynamics of ABP is driven by an exponentially correlated noise.

We simulated the Eq. (87) with $\eta(t) = 0$ on a semi-infinite line subject to the absorbing boundary condition at $x = 0$. We have taken random initial orientation such that $u_0 = 0$. The distribution at large times is captured remarkably well with $P^\infty(x, t) - P_{\text{BL}}$ given in Eqs. (79)-(80), with $D_e = \frac{v^2}{2D_r}$, $l_M \approx 0.8 \frac{v}{D_r}$. The result is shown in Figure 9. This corroborates the proposed universality of the large time

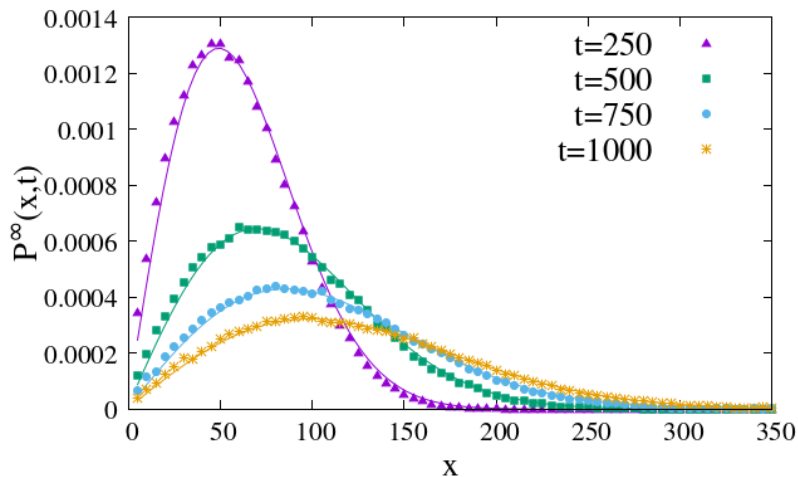


Figure 9: Distribution of athermal ABPs on a semi-infinite line with an absorbing barrier at $x = 0$. The data is shown with particle parameters $v = \sqrt{2}$, $D_r = 0.2$ and initial condition $x_0 = 1.0$, $u_0 = \langle \cos(\theta(0)) \rangle \approx 0$. The line corresponds to the expression in Eq. (79) except the boundary layer contribution.

distribution. Note that $P(x, t)$ has a discontinuity at $x = 0$. Since the noise is continuous-valued, we expect a boundary layer to be present that will alter the expression of the distribution near $x = 0$. This is however not taken in this paper.

References

- [1] S. Ramaswamy, *The mechanics and statistics of active matter*, Annu. Rev. Condens. Matter Phys. **1**, 310 (2010).

- [2] M. C. Marchetti, J.-F. Joanny, S. Ramaswamy, T. B. Liverpool, J. Prost, M. Rao, and R. A. Simha, *Hydrodynamics of soft active matter*, Rev. Mod. Phys. **85**, 1143 (2013).
- [3] C. Bechinger, R. Di Leonardo, H. Löwen, C. Reichhardt, G. Volpe, and G. Volpe, *Active particles in complex and crowded environments*, Rev. Mod. Phys. **88**, 045006 (2016).
- [4] J. R. Howse, R. A. L. Jones, A. J. Ryan, T. Gough, R. Vafabakhsh, and R. Golestanian, *Self-motile colloidal particles: From directed propulsion to random walk*, Phys. Rev. Lett. **99**, 048102 (2007).
- [5] Jiang, H.-R., N. Yoshinaga, and M. Sano, *Active motion of a Janus particle by self-thermophoresis in a defocused laser beam*, Phys. Rev. Lett. **105**, 268302 (2010).
- [6] N. Kumar, S. Ramaswamy, and A. K. Sood, *Symmetry properties of the large-deviation function of the velocity of a self-propelled polar particle*, Phys. Rev. Lett. **106**, 118001 (2011).
- [7] A. Murali, P. Dolai, A. Krishna, K. V. Kumar and S. Thutupalli, *Geometric constraints alter the emergent dynamics of an active particle*, Phys. Rev. Research. **4**, 013136 (2022).
- [8] J. Tailleur and M. E. Cates, *Statistical mechanics of interacting run-and-tumble bacteria*, Phys. Rev. Lett. **100**, 218103 (2008).
- [9] M. E. Cates and J. Tailleur, *Motility-induced phase separation*, Annu. Rev. Condens. Matter Phys. **6**, 219 (2015).
- [10] Y. Fily and M. C. Marchetti, *Athermal phase separation of self-propelled particles with no alignment*, Phys. Rev. Lett. **108**, 235702 (2012).
- [11] N. Kumar, H. Soni and S. Ramaswamy, *Flocking at a distance in active granular matter*, Nat Commun. **5**, 4688 (2014).
- [12] D. Ray, C. Reichhardt, and C. J. Olson Reichhardt, *Casimir effect in active matter systems*, Phys. Rev. E, **90**, 013019 (2014).
- [13] K. Malakar, V. Jemseena, A. Kundu, K. V. Kumar, S. Sabhapandit, S. N. Majumdar, S. Redner and A. Dhar, *Steady state, relaxation and first-passage properties of a run-and-tumble particle in one-dimension*, J. Stat. Mech. 043215 (2018).

- [14] A. Dhar, A. Kundu, S. N. Majumdar, S. Sabhapandit and G. Schehr, *Run-and-tumble particle in one-dimensional confining potentials: Steady-state, relaxation, and first-passage properties*, Phys. Rev. E, **99**, 032132 (2019).
- [15] S. C. Takatori, R. De Dier, J. Vermant, and J. F. Brady, *Acoustic trapping of active matter*, Nat. Commun. **7**, 10694 (2016).
- [16] K. Malakar, A. Das, A. Kundu, K. V. Kumar, A. Dhar, *Steady state of an active Brownian particle in a two-dimensional harmonic trap*, Phys. Rev. E, **101**, 022610 (2020).
- [17] P. Le Doussal, S. N. Majumdar and G. Schehr, *Velocity and diffusion constant of an active particle in a one-dimensional force field*, Europhys. Lett. **130**, 40002 (2020).
- [18] C. G. Wagner, M. F. Hagan, and A. Baskaran, *Response of active Brownian particles to boundary driving*, Phys. Rev. E, **100**, 042610 (2019).
- [19] A. Duzgun and J. V. Selinger, *Active Brownian particles near straight or curved walls: Pressure and boundary layers*, Phys. Rev. E, **97**, 032606 (2018).
- [20] Y. Fily, A. Baskaran and M. F. Hagan, *Pressure is not a state function for generic active fluids*, Nat. Phys. **11**, 673 (2015).
- [21] R. Ni, C. Stuart, A. Martien and P. G. Bolhuis, *Tunable long range forces mediated by self-propelled colloidal hard spheres*, Phys. Rev. Lett. **114**, 018302 (2015).
- [22] Y. Baek, P. A. Solon, X. Xu, N. Nikola and Y. Kafri, *Generic long-range interactions between passive bodies in an active fluid*, Phys. Rev. Lett. **120**, 058002 (2018).
- [23] J. Rodenburg, S. Paliwal, M. de Jager, P. G. Bolhuis, M. Dijkstra and R. van Roij, *Ratchet-induced variations in bulk states of an active ideal gas*, J. Chem. Phys. **149**, 174910 (2018).
- [24] Y. Fily, A. Baskaran and M. F. Hagan, *Dynamics and density distribution of strongly confined noninteracting nonaligning self-propelled particles in a non-convex boundary*, Phys. Rev. E, **91**, 012125 (2015).
- [25] C. G. Wagner, M. F. Hagan and A. Baskaran, *Steady-state distributions of ideal active Brownian particles under confinement and forcing*, J. Stat. Mech. 043203 (2017).

- [26] A. Das , A. Dhar and A. Kundu, *Gap statistics of two interacting run and tumble particles in one dimension*, J. Phys. A: Math. Theor., **53**, 345003 (2020).
- [27] A. Chugh and R. Ganesh, *Role of translational noise on current reversals of active particles on ratchet*, Sci. Rep. **13**, 16154 (2023).
- [28] D. Levis and L. Berthier, *Clustering and heterogeneous dynamics in a kinetic Monte Carlo model of self-propelled hard disks*, Phys. Rev. E, **89**, 062301 (2014).
- [29] T. Chakraborty, S. Chakraborti, A. Das and P. Pradhan, *Hydrodynamics, superfluidity, and giant number fluctuations in a model of self-propelled particles*, Phys. Rev. E, **101**, 052611 (2020).
- [30] L. Bertini and G. Posta, *Boundary driven Brownian gas*, ALEA, Lat. Am. J. Probab. Math. Stat., **16**, 361 (2019).
- [31] L. Bertini, A. De Sole, D. Gabrielli, G. Jona-Lasinio, and C. Landim, *Macroscopic fluctuation theory*, Rev. Mod. Phys. **87**, 593.
- [32] H. Spohn, *Long range correlations for stochastic lattice gases in a nonequilibrium steady state*, J. Phys. A **16**, 4275 (1983).
- [33] K. Mallick, *The exclusion process: A paradigm for non-equilibrium behaviour*, Physica A **418**, 17 (2015).
- [34] B. Derrida, M. R. Evans, V. Hakim, and V. Pasquier, *Exact solution of a 1D asymmetric exclusion model using a matrix formulation*, J. Phys. A **26**, 1493 (1993).
- [35] *Thermal Transport in Low Dimensions*, S. Lepri, Springer Cham, Cham, Switzerland (2016).
- [36] G. T. Landi, D Poletti and G. Schaller, *Nonequilibrium boundary-driven quantum systems: Models, methods, and properties*, Rev. Mod. Phys. **94**, 045006 (2022).
- [37] A. Dhar, A. Kundu and A. Kundu, *Anomalous Heat Transport in One Dimensional Systems: A Description Using Non-local Fractional-Type Diffusion Equation*, Front. Phys. **7**, 159 (2019).
- [38] A. Dhar, K. Saito and B. Derrida, *Exact solution of a Lévy walk model for anomalous heat transport*, Phys. Rev. E, **87**, 010103 (2013).

- [39] I. Santra, U. Basu, *Activity driven transport in harmonic chains*, SciPost Phys. **13**, 041 (2022).
- [40] R. Sarkar, I. Santra, U. Basu, *Stationary states of activity-driven harmonic chains*, Phys. Rev. E **107**, 014123 (2023).
- [41] P. Singh, S. Santra and Anupam Kundu, *Extremal statistics of a one-dimensional run and tumble particle with an absorbing wall*, J. Phys. A, **55**, 465004 (2022).
- [42] C.D. Pagani, *Study of some issues concerning the generalised Fokker-Planck equation*, Boll. Un. Mat. Ital. (4) **3** : 961 (1970).
- [43] M. A. Burschka and U. M. Titulaer, *The kinetic boundary layer for the Fokker-Planck equation: selectively absorbing boundaries*, J. Stat. Phys. **26**, 59 (1981).
- [44] U. M. Titulaer, *The Density Profile for the Klein-Kramers Equation Near an Absorbing Wall*, J. Stat. Phys. **37**, 589 (1984).
- [45] The zero magnetisation boundary condition, although quite similar to the passive case, is not very obvious or natural for the active system. For example, consider the reservoir to be constructed as a closed box of infinite spatial extent with reflecting walls at the two ends that contains noninteracting RTPs. Analytical results [13] show that an exponential layer, similar in form to the ‘kinetic boundary layer’, will appear. The strength of the layer falls with the box size, but for having a nonzero density at the edge where we shall connect it with the system, the number of particles must go to infinity in proportion to the box size, and that would in turn give a nonzero Q_0 and Q_1 . In general, the boundary magnetisation is expected to depend on the construction of the reservoir or the reservoir-system coupling.
- [46] The approximation carries a tiny error $\sim O(e^{-\mu L})$. Note the importance of keeping l_M in the denominator for the accuracy of the approximation.
- [47] T. W. Marshall and E. J. Watson, *The analytic solutions of some boundary layer problems in the theory of Brownian motion*, J. Phys. A: Math. Gen. **20**, 1345 (1987).
- [48] A nonzero Milne length implies that the particle far from the boundary sees the absorbing condition at $x = -l_M$ instead of $x = 0$. However in Eq. (73) or Eq. (79), the quantity $P_{\text{tr}}^\infty - P_{\text{BL}}$ doesn’t exactly vanish at $-l_M$ and is off from zero by a tiny amount $\sim l_M^2 t^{-3/2}$ or $l_M u_0 \tau_p t^{-3/2}$. One can show that for RTP such terms occur from $O(L^{-2})$ corrections in the large- L expansion

of the spectrum (section 4.3), and are therefore omitted. Note that, at large times $\sqrt{D_e t} \gg u_0 \tau_p, l_M, P_{\text{BM}}$ and P_{CS} in Eq. (79) can be combined to write, $P_{\text{tr}}^\infty(x, t; x_0) - P_{\text{BL}} \approx \frac{1}{\sqrt{4\pi D_e t}} \left[\exp\left\{-\frac{(|x-x_0| \pm u_0 \tau_p)^2}{4D_e t}\right\} - \exp\left\{-\frac{(x+x_0+2l_M+u_0 \tau_p)^2}{4D_e t}\right\} \right]$, where \pm is for $x \lesseqgtr x_0$ respectively. This particular form is exactly obtained in the underdamped case (Eq. (85)).

- [49] P. Dolai, A. Das, A. Kundu, C. Dasgupta, A. Dhar, K. V. Kumar, *Universal scaling in active single-file dynamics*, *Soft Matter*, **16**, 7077 (2020).
- [50] E. Fodor, C. Nardini, M. E. Cates, J. Tailleur, P. Visco, and F. Van Wijland, *How Far from Equilibrium Is Active Matter?*, *Phys. Rev. Lett.* **117**, 038103 (2016).
- [51] B. Ezhilam, R. A.-Matilla, and D. Saintillan, *On the distribution and swim pressure of run-and-tumble particles in confinement*, *J. Fluid Mech* **781**, R4 (2015).
- [52] M. C. Wang and G. E. Uhlenbeck, *On the Theory of the Brownian Motion II*, *Rev. Mod. Phys.* **17**, 323 (1945).
- [53] T. W. Marshall and E. J. Watson, *A drop of ink falls from my pen... it comes to earth, I know not when*, *J. Phys. A: Math. Gen.* **18**, 3531 (1985).
- [54] J. V. Selinger and U. M. Titulaer, *The kinetic boundary layer for the Klein-Kramers equation; A new numerical approach*, *J. Stat. Phys.* **36**, 293 (1984).